Advanced Review

Chemical looping technology for energy and chemical production

Samuel C. Bayham, Andrew Tong, Mandar Kathe and Liang-Shih Fan*

Chemical looping has been considered as a promising technology for CO_2 capture and for producing electricity and/or chemicals from various carbonaceous feedstocks. This article provides an overview of chemical looping processes, their potential process configurations, and applications for power and chemical production. The designs and results of various demonstration units are discussed in relation to parameters required for commercialization. Furthermore, the barriers to commercialization of a chemical looping plant for power or syngas production are illustrated.

How to cite this article:
WIREs Energy Environ 2016, 5:216–241. doi: 10.1002/wene.173

INTRODUCTION

In 1987, Ishida et al. first coined the term 'chemical looping' for processes that use a metal oxide intermediate to perform a redox reaction scheme as an alternative means of combustion for increased exergy efficiency in power production.[1] The use of metal oxides in redox reaction can be traced back as far as the 1900s with the Howard Lane Hydrogen Producer process[2,3] Later manifestations of the idea were proposed for CO_2 production from carbonaceous fuels using copper or iron oxides in the processes developed by Lewis and Gilliland.[4] In recent years, there has been an exponential growth of research and publications in this field, and the scope of chemical looping has broadened to encompass the use of chemical looping for partial oxidation to produce syngas for chemicals production. Metal oxides of iron, nickel, and copper are most commonly used as the chemical intermediates where their oxidation state swings within each subreaction. Decomposing the single combustion reaction produces concentrated products without the need for further separation techniques. Additionally, in the case of power production, the use of the chemical intermediate increases the reversibility of the combustion reaction, thereby, increasing the exergy efficiency of the overall process.

This article provides an overview of chemical looping processes, their potential process configurations, and applications for power and chemical production. Results from various demonstration units are also discussed in relation to parameters required for commercialization. Furthermore, the barriers to commercialization of a chemical looping plant for power or syngas production are elaborated.

Motivations

Currently, cheap, abundant energy sources are necessary to meet growing demands for power and chemicals. Predictions show that an increase in atmospheric CO_2 to 450–600 ppmv may result in increased average earth temperatures and extreme weather phenomena.[5,6] As world population increases and nations further undergo industrialization, it is expected that primary energy usage will increase, particularly in non-OEDC countries such as China and India.[7] Hydrogen is a major constituent required for chemicals and petrochemicals production and has also been proposed as an alternative transportation fuel as the only emission is water vapor.[8] Presently, hydrogen is produced from the catalytic reforming of natural gas, via steam, partial oxidation, or autothermal reforming. The total CO_2 emitted per cubic meter of hydrogen is approximately 0.426 kg using these reforming processes.[9] Assuming a natural gas price of $2.99/GJ, a typical hydrogen selling price

*Correspondence to: fan.1@osu.edu

William G. Lowrie Department of Chemical and Biomolecular Engineering, Koffolt Labs, The Ohio State University, Columbus, OH, USA

Conflict of interest: The authors have declared no conflicts of interest for this article.

for a steam-methane reforming process is around $5.25/GJ, and due to the dilute concentration of the CO_2 emitted from steam-methane reforming, this cost can increase by 15–28%[10,11] Chemical looping for power and chemical production has the potential for *in situ* CO_2 capture eliminating the need for energy intensive gas-gas separation techniques.

In the case of power production, the chemical looping scheme theoretically allows for high exergetic efficiency, as the high grade heat produced from the oxidation of the oxygen carrier can be extracted for steam production, while the lower grade heat is recuperated in the oxygen carrier to perform its endothermic reduction. Originally, Richter and Knoche[12] and Ishida et al.[1] intended to reduce the exergy loss in a power plant system that utilizes a gas turbine by using the chemical looping scheme in lieu of a conventional fuel combustor.[13] Because the combustion temperature and exergy loss are lower in the chemical looping combustor system proposed by Ishida et al. compared to traditional combustion, the gas turbine could be designed for lower temperatures with more cost-effective materials.[13] However, the heat integration scheme involved in the CLC system proposed by Ishida et al. uses high-temperature gas–solid heat exchangers and low reducer temperatures, which may be impractical for an actual chemical looping power plant. Nevertheless, the chemical looping combustion (CLC) scheme that does not utilize high-temperature gas–solid heat exchangers but allows for *in situ* carbon capture has a greater process efficiency than a conventional combustion system that performs the carbon dioxide separation as a postcombustion step.[14]

Chemical Looping Process Applications

For chemical looping systems, the carbonaceous fuel enters the reduction step where it reacts with a metal oxide or sulfate to become either partially oxidized to synthesis gas or fully oxidized to CO_2 and steam. The reduced metal oxide/sulfate is sent to another reactor for oxidation. Here, steam or air is used to produce hydrogen or oxygen-depleted air, respectively. The oxidation step is usually exothermic resulting in energy released for power production. This is different than carbonate looping systems, where alkali or alkaline earth metal oxides react with CO_2 in gas streams to form metal carbonates. In such systems, the metal carbonates are calcined in a separate reactor to form concentrated CO_2 that can be sequestered or utilized, Carbonate systems are being researched for post- and pre-combustion applications. Many review publications have been presented on carbonate looping systems,[15,16] and this article will only focus on chemical looping systems.

A number of advancements in the chemical looping scheme have resulted in increased process efficiency and economic benefit for carbon capture over traditional systems. The most studied applications include the conversion of carbonaceous fuels to electricity, hydrogen, and quality syngas for Fisher-Tropsch or methanol production. Smaller scale chemical looping applications include an alternative air separation scheme[17] and removal of ventilation air methane (VAM) for mining operations.[18]

CHEMICAL LOOPING FOR POWER PRODUCTION WITH CO_2 CAPTURE

Chemistry

The intent of CLC is to completely oxidize fuel to carbon dioxide and steam while producing heat for power production. In the reducer reactor, also known as the fuel reactor, the overall reaction of a generic metal oxide, MO_x, with a generic hydrocarbon $C_aH_bO_c$ is:

$$C_aH_bO_{c(g,l,s)} + MO_{x(s)} = aCO_{2(g)} + bH_2O_{(g)} + MO_{y(s)}, \quad (1)$$

where $y = x + c - 2a - b/2$. This reaction can be either endothermic or slightly exothermic, depending on the metal oxide and reactant gas composition.

Regeneration of the oxygen carrier occurs in a combustor, also known as the air reactor, using the following reaction:

$$MO_y + O_2 = MO_x. \quad (2)$$

This reaction is usually exothermic, releasing energy that can be extracted from the solids or the spent air to generate steam for electricity generation. If the CLC process is operated at elevated pressure, the combustor can be integrated with a gas turbine as part of a Brayton cycle. Advanced CLC integration systems are further discussed in *Advanced Configurations and Process Simulation for Power Production* section.

A number of fuels have been considered for CLC applications, such as syngas, natural gas, coal, petroleum coke, liquid resid, and biomass. Gaseous fuels react directly with the oxygen carrier as shown in Reaction 1, but for solid fuel CLC processes, the reaction kinetics between the oxygen carrier and the fuel are unfavorably slow. Two possibilities have been developed to overcome this challenge. The first option is to gasify the solid fuel *in situ* with the oxygen carrier using an enhancer gas to perform a gas-solid reaction. The gaseous products then react with the metal oxide to form CO_2 and H_2O as in Reaction 1. Usually steam or carbon dioxide is used as the enhancer gas to minimize costs and prevent product gas dilution. The

steam and carbon dioxide are products of Reaction 1, so a slipstream of the flue gas is recycled back to the reducer. The main reactions behind gasification enhancement of the devolatilized coal char are the water gas and Boudouard reactions[19,20]:

$$C_{(s)} + H_2O_{(g)} = CO_{(g)} + H_{2(g)}. \quad (3)$$

$$C_{(s)} + CO_{2(g)} = 2\,CO_{(g)}. \quad (4)$$

The second option for solid fuel CLC is to use an oxygen carrier that has the ability to produce molecular oxygen the reducer. The reaction for this metal oxide is:

$$MO_{x(s)} = MO_{x-2(s)} + O_{2(g)}. \quad (5)$$

The molecular oxygen can then directly oxidize the solid coal char and volatiles in the following reaction:

$$C_aH_bO_{c(g,s)} + yO_{2(g)} = aCO_{2(g)} + b/2\,H_2O_{(g)}, \quad (6)$$

where $y = 4a + b - 2c$. This scheme is called chemical looping oxygen uncoupling (CLOU). Common oxygen carriers used in CLOU processes include CuO, Mn_3O_4, and CoO.[21–23] The advantage of CLOU is its ability to convert less reactive fuels, such as petroleum coke, resulting in a shorter solids residence time in the reducer.[24] However, the oxygen carrier material needs to be carefully selected such that its equilibrium partial pressure is below that required for regeneration in air. A disadvantage of CLOU is the possibility of emitting unconverted oxygen in the CO_2 stream, resulting in incompliance with some pipeline specifications.[25]

Reactor Design for Power Production

The design of a CLC system must consider conversion of the fuel and oxygen carrier, reactor hydrodynamics, and solids handling. For *in situ* gasification of solid fuels, sufficient knowledge of the char gasification rate and its hydrodynamics is necessary to properly design the reducer for complete fuel conversion and carbon capture, the gas–solid separation equipment, and the char/ash-oxygen carrier stripping devices. Furthermore, practical devices for preventing combustor and reducer gases from mixing need to be designed.

Reducer Design Characteristics

In the reducer, the oxygen carrier and fuel contact time should be sufficient to completely convert the fuel to CO_2 and steam, with minimal combustibles remaining in the outlet stream. The conversion is primarily a function of gas velocity and bed height, but other factors include the gas-solid contacting pattern, the degree of gas channeling in the bed, and external mass transfer limitations. The choice of contacting pattern for metal oxides that exhibit more than two oxygen states, such as oxides of iron or manganese, should also consider thermodynamics.[26,27] While all chemical looping reducer designs are different, they can generally be classified into two groups: Mode I, consisting of a fluidized or cocurrent-flow packed bed, and Mode II, consisting of countercurrent fuel and oxygen carrier flow such as that found in a moving packed bed or multistage fluidized beds in series. This designation is shown in Figure 1. For Mode I fluidized bed operation, the gas flow through the reducer must be greater than the minimum fluidization velocity, U_{mf}. When converting gaseous fuels, the fuel feedstock can be used to maintain the oxygen carrier fluidization. In solid fuel systems, an additional fluidization gas must be used to fluidize both the oxygen carrier and solid fuel. For Mode II counter-current chemical looping systems, a larger oxygen carrier particle size and density can be used as the gas flow must be maintained below the U_{mf} of the oxygen carrier. Thus, Geldart group D particle is used for Mode II as opposed to Geldart group A particles for Mode I operation. In Mode II chemical looping systems for solid fuel conversion, the oxygen carrier size generally is an order of magnitude greater than the solid fuel ash size, greatly simplifying the solid–solid separation required for ash removal.

The disadvantage of Mode I reducers for CLC systems is that the driving force for metal oxide reduction reaction is inversely related to the fuel conversion to CO_2/H_2O. In Mode I, fresh oxygen carrier is introduced with high partial-pressure fuel gas, but as the reaction proceeds, the oxygen carrier conversion increases and the partial pressure of fuel gas decreases. As a result, the reaction rate decreases, which prevents efficient conversion of the fuel. The mixing nature of fluidized bed used in conjunction with Mode I further exacerbates this issue.

The counter-current Mode II reducer operation allows for full fuel conversion to CO_2/H_2O and high oxygen carrier reduction. As the fuel enters the reducer, the high partial pressures of the reducing gases allow for the oxygen carrier to be highly reduced. As illustrated in Figure 1, the fuel is partially oxidized and travels upward where the oxidized oxygen carrier particles polish the unconverted fuel to CO_2 and H_2O. Previous studies were performed comparing the Mode I and Mode II operation using iron based oxygen carriers with H_2 as the reducer fuel gas. The analysis was performed using the phase diagram of the oxidation states of iron and the oxygen balance between the oxygen carrier and fuel. The results showed that

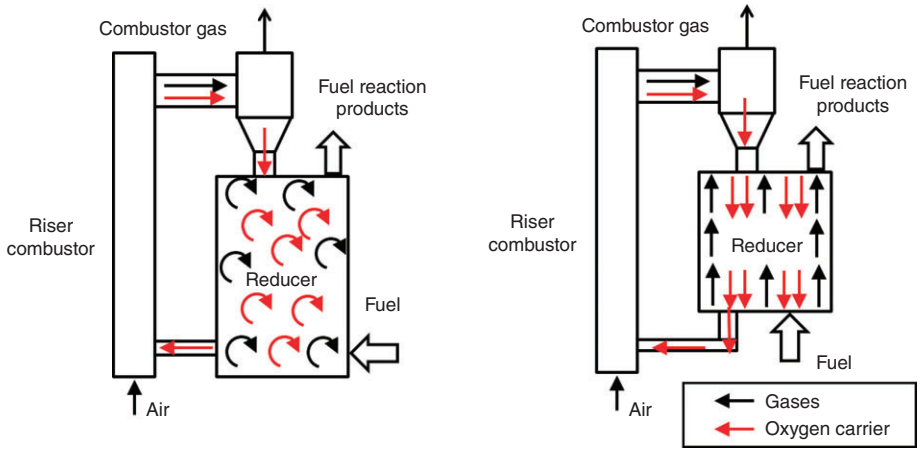

FIGURE 1 | Modes of chemical looping: (a) Mode I: well mixed single stage reducer and (b) Mode II: countercurrent multistage reducer.

when restricting the product gas to complete fuel conversion, the maximum achievable oxygen carrier conversion was 11% (or Fe_3O_4 oxidation state) and 50% (or Fe and FeO oxidation states) for Mode I and Mode II reducer operations, respectively. The oxygen carrier conversion as defined here is the number of moles of oxygen consumed by the carbonaceous fuel divided by the total moles of oxygen in the oxygen carrier.

One potential disadvantage of Mode II systems is the large temperature decrease in the reducer reactor due to the higher degree of reduction. While the degree of reduction in the reducer causes a greater temperature difference, this can be overcome through the following. First, the addition of a suitable support material of sufficient heat capacity helps to mitigate the reduction in temperature. A particle can also be designed that can take a higher temperature in the combustor, which would help to maintain the minimum reducer temperature above a point where the kinetics of gasification and particle reduction are reasonable. Second, while the char gasification reactions may be slower at lower temperatures, the larger size of the Geldart D particle can allow for interstitial fluidization of the char particle in between the oxygen carrier particles, which helps to extend the residence time of the char over that of the oxygen carrier particle. Furthermore, as the char particle continues to react and shrinks, it will flow through the top of the reducer, which is hotter than the lower sections that have been cooled through the endothermic reduction and gasification reactions.

Combustor Reactor and Sealing

The combustor design should take into account similar factors as that for the reducer, such as reaction kinetics and thermodynamics. As the reaction of air with reduced metal oxide is exothermic, heat should be well distributed throughout the bed to prevent particle melting or sintering, which can deactivate the particle and cause operability issues. Therefore, a fluidized bed is best, and proposed commercial designs take advantage of prior research performed for CFB combustion systems.[28] Additionally, excess air should be minimized to prevent excessive cooling of the oxygen carrier, as the energy from the oxygen carrier is required to sustain the reactions in the reducer. Heat can also be recuperated from the spent air with a convection pass.

Some combustor designs use a fast-fluidized bed, but the disadvantage is a short solids residence time if a suitable bottom bed is not maintained.[29] If a longer residence time is required, a larger-diameter bubbling fluidized bed is required to retain the particles. Particles exiting from the fluidized bed freeboard become entrained in a high-velocity riser. Two combustors in series may also be necessary, as in the 10-kW_{th} unit developed by Sozinho et al.[30]

For some designs, the riser gas velocity drives the solids circulation rate, such as the unit developed by Lyngfelt et al. Therefore, the combustor and riser can be used to control the solid flow rate. The combustor developed by Kolbitsch et al. operates in either the dilute or dense transport regime.[31] Primary and secondary air injection is used. The system solids circulation rate is controlled by throttling both air flows in the combustor. When the overall air flow rate is fixed, a larger primary air flow rate produces a higher solids circulation rate. Splitting the air demands strategically can allow for a higher temperature at the bottom of the riser for enhanced heat recovery.

Furthermore, an appropriate method of preventing air from mixing with the reducer gases is required. Many of the designs shown in Figures 2–8 use loop seals fluidized with steam or CO_2. The diameter of the

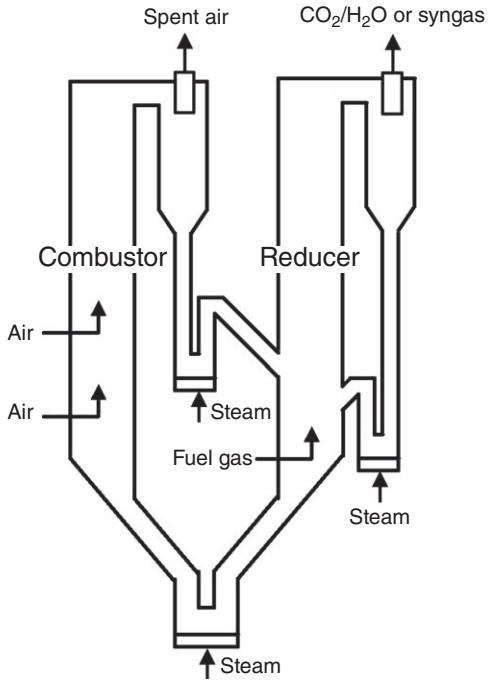

FIGURE 2 | Chemical looping combustion/reforming unit developed by Proll et al.

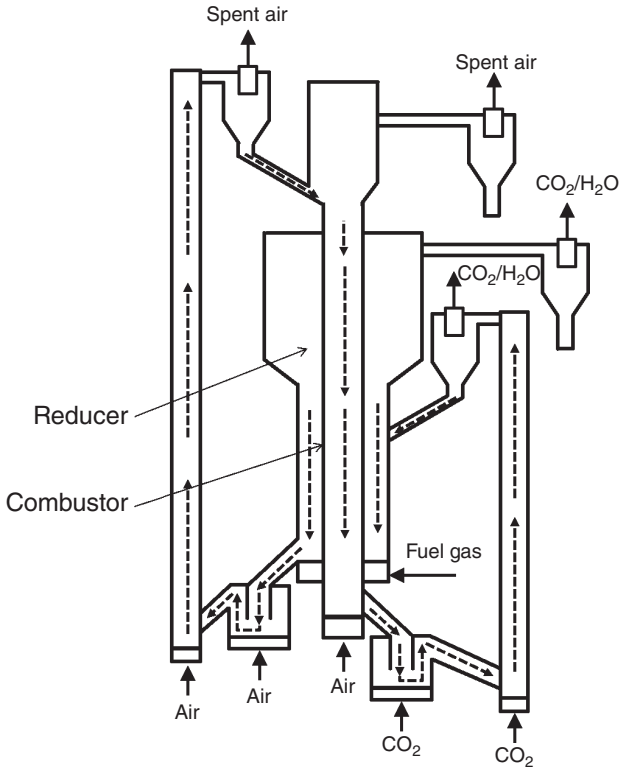

FIGURE 3 | Chemical looping system developed by Son and Kim.

loop seal piping should be narrow enough to minimize the amount of sealing gas are required, yet it should be large enough to allow for solids to flow without operational issues. The unit developed by Shen et al. does not have a loop seal between the top of the reducer and the spent air cyclone. The higher pressure caused by the standpipe inventory of the returned solids from the air cyclone causes the CO_2/H_2O to exit the reducer and not backflow through the cyclone.

Several Mode I and Mode II chemical looping process designs for gaseous fuel and solid fuel conversion are presented in the following sections. A summary of the designs for various chemical looping pilot facilities is shown in Table 1.

Gaseous Fuel Chemical Looping

Several processes use the fluidized bed Mode I concept for the reducer design. A 10-kW_{th} gaseous fuel unit by Lyngfelt et al. consists of a bubbling fluidized bed reducer, with dimensions based on the range of velocities for oxygen carrier elutriation and minimum fluidization,[32] while the height was set by the known residence time requirements of the fuel and oxygen carrier reaction. The region above the freeboard also consists of an expanded section to account for increased gas flow from methane conversion. A similar 10-kW unit developed by Adanez et al. also operates under bubbling fluidized bed conditions with overflow exits.[33] A smaller 500-W_{th} system constructed by Adanez et al. and a 300-W_{th} system were designed similarly to test smaller batches of oxygen carriers.[34,35]

Several Mode-II systems were developed to provide better conversions. A 120-kW_{th} dual-circulating fluidized bed (DCFB) system designed by Kolbitsch et al.[36] is shown in Figure 2. Fuel is injected from the bottom of the turbulent fluidized bed, and two oxygen carrier streams are introduced to the reducer. Fresh particles from the combustor are introduced into the middle of the reducer to ensure high fuel conversion, while the partially reduced oxygen carrier that is separated from the cyclone at the top of the reducer is returned to the bottom near the region of fuel injection to increase the oxygen carrier reduction. The 1-kW_{th} system shown in Figure 3 developed by Son and Kim for methane conversion consists of a Mode II reducer, which exists as the outer concentric pipe.[37] The reducer in the 50-kW_{th} system developed by Ryu et al. also consists of a downward flow fluidized bed.[38]

Solid Fuel Chemical Looping

Designing a reducer for complete solid fuels conversion introduces greater challenges than gaseous fuel conversion, as the hydrodynamics of the coal char need to be taken into account along with the oxygen carrier. A fluidized bed allows the solid fuel and

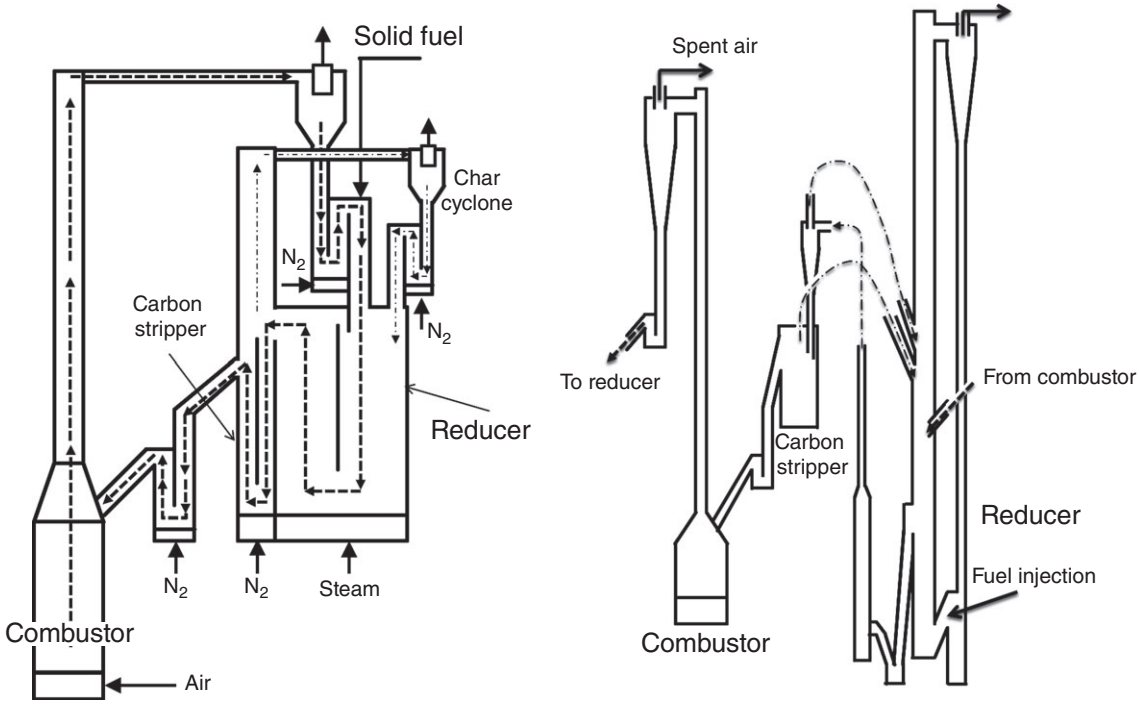

FIGURE 4 | Chemical looping system developed by Lyngfelt et al. for solid fuel conversion: (a) 10-kW_{th} unit and (b) 100-kW_{th} unit.

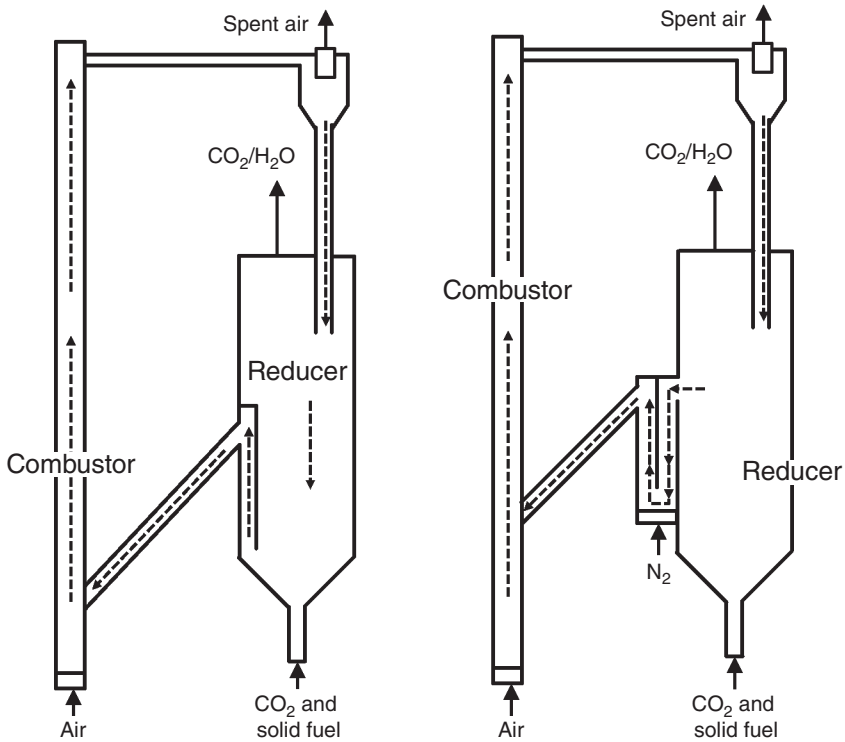

FIGURE 5 | Chemical looping system developed by Shen et al. for solid fuel conversion: (a) 10-kW_{th} unit and (b) 1-kW_{th} unit.

oxygen carrier to be well-mixed, but the fluidized bed has the potential to cause the fuel char to elutriate out before it is fully converted. Research groups using fluidized bed reducers have attempted to prevent this issue by modifying the standard fluidized bed design.

Lyngfelt et al. developed a Mode I reducer sized for 10-kW_{th} fuel input that consists of multiple sections, as shown in Figure 4(a) to narrow the residence time distribution by promoting the plug flow of solids and char. Fuel conveyed into the top of the

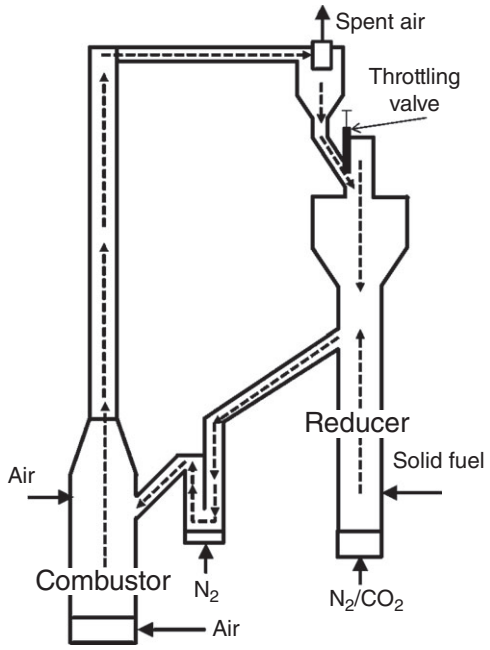

FIGURE 6 | Chemical looping system developed by Abad et al. for solid fuel conversion.

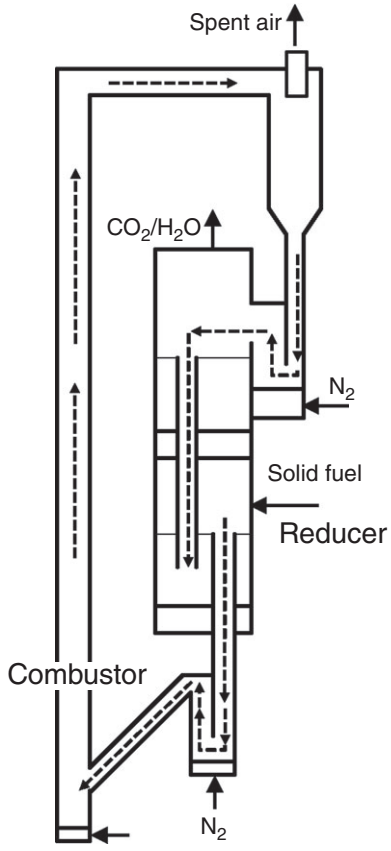

FIGURE 7 | Chemical looping system developed by Thon et al. for solid fuel conversion.

reducer mixes with fresh oxygen carrier. Injection of the fuel occurs below the surface of the bed to prevent short-circuiting of the volatiles.[39] The mixture flows through three distinct sections: (1) a low velocity gas section, where volatile gases are driven off; (2) a high velocity section, where remaining solid fuel reacts with oxygen carrier; and (3) a carbon stripper section, where residual fuel is separated from the oxygen carrier. The gases and fines that exit from the carbon stripper are sent through a cyclone that separates the oxygen carrier from the unreacted fuel and ash. Steam flows in the high velocity section to gasify the fuel, fluidize the particle, and promote mixing of fuel and oxygen carrier.

The spouted fluidized bed reducer design for the 10-kW_{th} integrated CLC unit developed by Shen et al. shown in Figure 5(a) was chosen to allow for a long fuel-char residence time. Solid fuel and CO_2 are injected together from the bottom, and the spouted mixture of oxygen carrier and char flow downwards along the edge where they also exit. A 1-kW_{th} unit was later designed, shown in Figure 5(b), to allow the oxygen carrier to exit from the top of the reducer instead of the bottom, which prevents CO_2 from entering the combustor. For both designs, fresh oxygen carrier from the combustor enters the top of the bed through a standpipe. While the fluidized bed is unspouted, the 1.5-kW_{th} reducer developed by Abad et al. is similar to that of Shen et al., except it contains a disengagement zone above the freeboard, as shown in Figure 6.[40] These units also do not contain a carbon stripper.

The reducer for the 100-kW_{th} unit developed by Lyngfelt et al., shown in Figure 4(b), is a CFB.[41] Fresh oxygen carrier along with recycled char and fines from the carbon stripper is introduced into the middle of the fluidized bed. Fuel is introduced into the bottom loop seal and flows upwards with the fluidized bed of oxygen carrier. The reduced oxygen carrier exits the middle of the reducer, enters another loop seal, and becomes entrained into a carbon stripper. For the 1-MW_{th} unit developed by Epple et al., pulverized coal enters the bottom of the reducer, where it is added to the fluidized bed of oxygen carrier, and the flue gas exits out from two cyclones connected in series.[42] The first cyclone is a low-efficiency cyclone designed to capture the heavy particles, which are sent to the carbon stripper. The gas outlet from the first cyclone is sent to a high efficiency cyclone to separate out the powders, which are recycled back to the coal inlet. The unconverted fuel entering the carbon stripper is removed using steam and CO_2. A 50-kW_{th} CLOU unit (20-kW_{th} for CLC operation) developed by Perez-Vega has a similar DCFB design.[43]

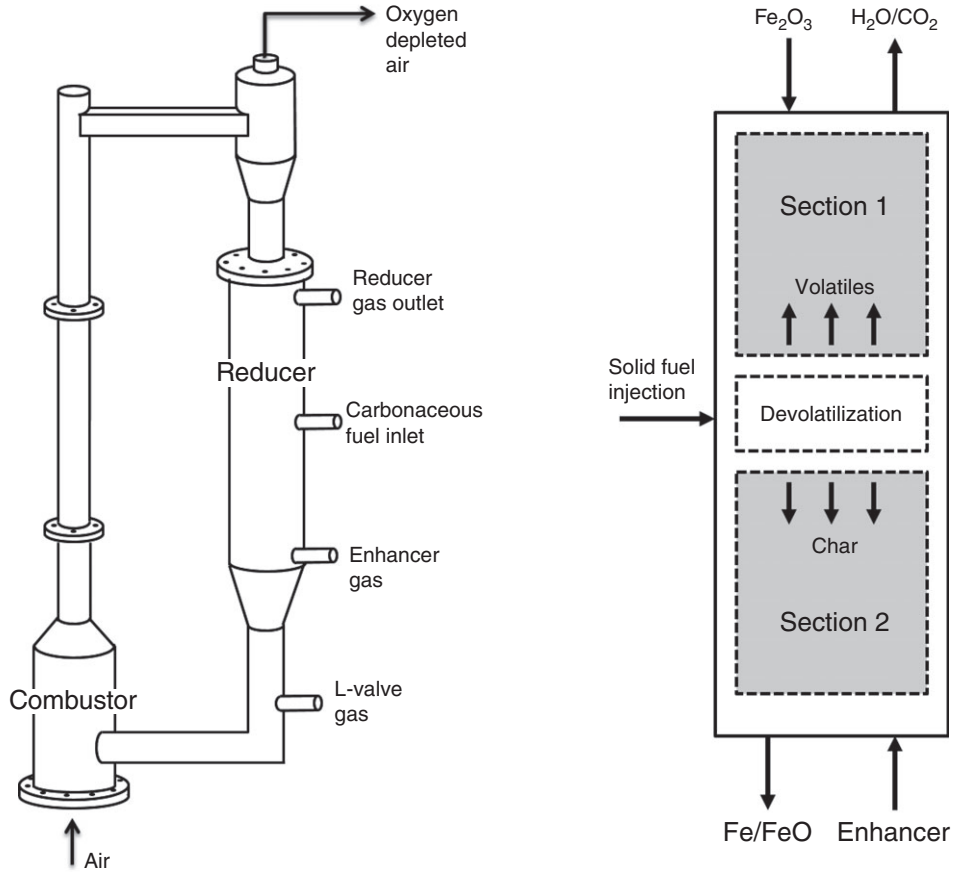

FIGURE 8 | (a) Chemical looping system developed by Fan et al. for solid fuel conversion and (b) reducer design.

To allow for higher volatile conversion, other designs provide sufficient residence time for gaseous products above the fuel injection region. The reducer developed by Thon et al. was designed as a two-stage fluidized bed with overflow standpipes, as shown in Figure 7.[44] Coal is introduced into the bottom of the first reducer where CO_2 is used to fluidize the solids. The volatiles and gasification products produced at the bottom of the reactor fluidize the top bed, and the reacted oxygen carrier enters the overflow standpipe into the top fluidized bed. An overflow standpipe transfers the oxygen carrier from the top into the bottom fluidized bed.

The reducer developed by Fan et al. shown in Figure 8(a) uses a Mode-II moving bed design to optimize char and oxygen carrier conversion.[45,46] Fresh Fe_2O_3 enters the top of the reducer and travels countercurrent to the gas flow. Fuel is fed into the middle of the reducer as illustrated in Figure 8(b). In section 1, the volatiles and gasified products react counter currently with fresh oxygen carriers, polishing the product gas to high-purity CO_2. In section 2, char is gasified with steam and CO_2. The remaining ash fluidizes in the interstitial oxygen carrier space and is entrained out of the reducer in the CO_2 stream. The reducer design ensures full fuel conversion while achieving high oxygen carrier conversion, and ash is removed *in situ*.[46]

Oxygen Carrier Development

The oxygen carrier serves as the chemical intermediate to indirectly transfer pure oxygen from air to the fuel source via a redox reaction scheme. Multiple primary metal oxides and metal sulfates are considered for CLC process including, Ni, Fe, Mn, Cu, and $CaSO_4$. In the case of CLC, the metal oxide must be capable of fully converting the fuel source to concentrated CO_2 for carbon capture. Figure 9 illustrates a modified Ellingham diagram for the metal oxides considered. This diagram graphs the Gibbs free energy with temperature for the oxidation of the metal oxides and fuel (CO and H_2 in this case) with 1 mole of O_2. At a given temperature, the Gibbs free energy for the reaction of a metal oxide with CO can be determined by taking the difference of Gibbs free energy between the fuel and the metal oxide. Therefore, the metal oxide is capable of converting the fuel to CO_2

TABLE 1 | Summary of CLC System Designs, Oxygen Carriers, and Fuels Tested

Authors	Fuel Input	Reducer Design and Remarks	Combustor Design and Remarks	Carbon Stripper	Fuels Tested	Oxygen Carriers Tested
Lyngfelt et al.[32]	10 kW_{th} gaseous	Mode 1 bubbling fluidized bed; overflows to loopseal combustor. Disengagement zone above freeboard to allow for expansion while converting methane	Bubbling fluidized bed with riser	n/a	Natural gas, syngas	$NiO/NiAl_2O_4$; $Fe_2O_3/MgAl_2O_4$; $NiO/NiAl_2O_4/MgAl_2O_4$; $CaMn_{0.9}Mg_{0.1}O_{3-\delta}$; $CaMn_{0.775}Mg_{0.1}Ti_{0.125}O_{3-\delta}$
Lyngfelt et al.[39,56–58]	10 kW_{th} solid fuel	Mode 1 bubbling fluidized bed; consists of high velocity (HIVEL) and low velocity (LOVEL) sections for solid fuel devolatilization and gasification, respectively. Partitions allow for a more narrow residence time distribution solids	Bubbling fluidized bed with riser	Yes	Petroleum coke; bituminous coal; wood char	Ilmenite; manganese ores; ilmenite with lime; manganese with lime
Lyngfelt et al.[59–61]	100 kW_{th} solid fuel	Mode 1 circulating fluidized bed; oxygen carrier exits into an intermediate circulation riser before entering carbon stripper	Circulating fluidized bed	4 chamber carbon stripper	Petroleum coke, cerrejon coal	Ilmenite; manganese ore
Shen et al.[62,63]	10 kW_{th} solid fuel	Mode 2 spouted fluidized bed. Injection of fuel at bottom.	Fast fluidized bed	No	Biomass; coal.	NiO/Al_2O_3; Fe_2O_3
Shen et al.[64–67]	1 kW_{th} solid fuel	Mode 2 spouted fluidized bed. Injection of fuel at bottom.	Fast fluidized bed	No	Biomass; coal; waste sludge	NiO/Al_2O_3; Iron ore/CaO; Iron ore/CaO/Al_2O_3
Xiao et al.[107,108]	50 kW_{th} solid fuel, pressurized system	Mode 1 fast fluidized bed.	Turbulent fluidized bed	No	Bituminous coal	Iron ore
Thon et al.[44]	25 kW_{th} solid fuel	Mode 2 bubbling fluidized beds; bottom fluidized bed for char gasification and devolatilization; top fluidized bed for fuel volatiles conversion with overflow standpipe	Fast fluidized bed	No	Methane and coal.	CuO, ilmenite
Abad et al.[33]	10 kW_{th} gaseous fuel	Mode 1 bubbling fluidized bed with disengagement zone above freeboard	Bubbling fluidized bed and riser. Solids flow after combustor cyclone controlled by gate valve	No	Natural gas; syngas	CuO/Al_2O_3; NiO
Abad et al.[40]	1.5 kW_{th} solid fuels	Mode 1 bubbling fluidized bed with disengagement zone above freeboard	Bubbling fluidized bed and riser. Solids flow after combustor cyclone controlled by gate valve	No	Biomass, petroleum coke	$CuO/MgAl_2O_4$
Perez-Vega et al.[43]	50 kW_{th} CLOU (20 kW_{th} CLC) solid fuels	Mode 1 circulating fluidized bed	Circulating fluidized bed	Yes	lignite, bituminous coal; biomass	Ilmenite; $CuO/MgAl_2O_4$

TABLE 1 | Continued

Authors	Fuel Input	Reducer Design and Remarks	Combustor Design and Remarks	Carbon Stripper	Fuels Tested	Oxygen Carriers Tested
Son and Kim[37]	1 kW_{th}	Mode 2 bubbling fluidized bed in downflow	Bubbling fluidized bed in downflow	n/a	Methane	NiO with bentonite; Fe_2O_3 with bentonite
Ryu et al.[38]	50 kW_{th}	Mode 2 bubbling fluidized bed in downflow. Solids flow controlled by valve between reducer and combustor	Bubbling fluidized bed and riser	n/a	Methane	NiO/bentonite; CoO/Al_2O_3
Kolbitsch et al.[31,54,55]	120–140 kW_{th} gaseous fuel	Mode 2 turbulent fluidized bed; higher-conversion oxygen carrier recycled from cyclone to bottom of reducer; fresh oxygen carrier added at top of reducer	Fast fluidized bed with primary and secondary air injection	n/a	Methane; syngas	NiO and Al_2O_3; $(Fe,Mg)_2SiO_4$; Ilmenite; $NiO/Al_2O_3/MgO$; CuO/Al_2O_3; Fe_2O_3/Al_2O_3; $CaMn_{0.9}Mg_{0.1}O_{3-\delta}$; $CaMn_{0.775}Mg_{0.1}Ti_{0.125}O_{3-\delta}$
Epple et al.[42]	1 MW_{th}	Mode 1 circulating fluidized bed reactor with two cyclones in series	Circulating fluidized bed. Screw feeder drives solids to reducer	Yes	Hard coal	Ilmenite
Zheng et al.[109]	5 kW_{th}	Mode 1 bubbling fluidized bed	Fast fluidized bed	No	Bituminous coal	Ilmenite
Abduallaly et al.[110]	3 MW_{th}	Mode 1 circulating fluidized bed	Circulating fluidized bed	No	Bituminous coal;	$CaSO_4$ with $CaCO_3$
Fan et al.[96]	25 kW_{th} gaseous fuels	Mode 2 countercurrent moving bed reducer with oxidizer	Bubbling fluidized bed and riser	n/a	Syngas, methane	Fe_2O_3 based oxygen carrier
Fan et al.[45]	25 kW_{th} solid fuels	Mode 2 countercurrent moving bed	Bubbling fluidized bed and riser	No	Lignite, sub-bituminous, bituminous, metallurgical coke, biomass	Fe_2O_3 based oxygen carrier
Sozinho et al.[30]	10 kW_{th} solid fuel	Mode 2 countercurrent bubbling fluidized bed	Two bubbling fluidized bed combustors in series	Yes	Bituminous coal	Manganese ore

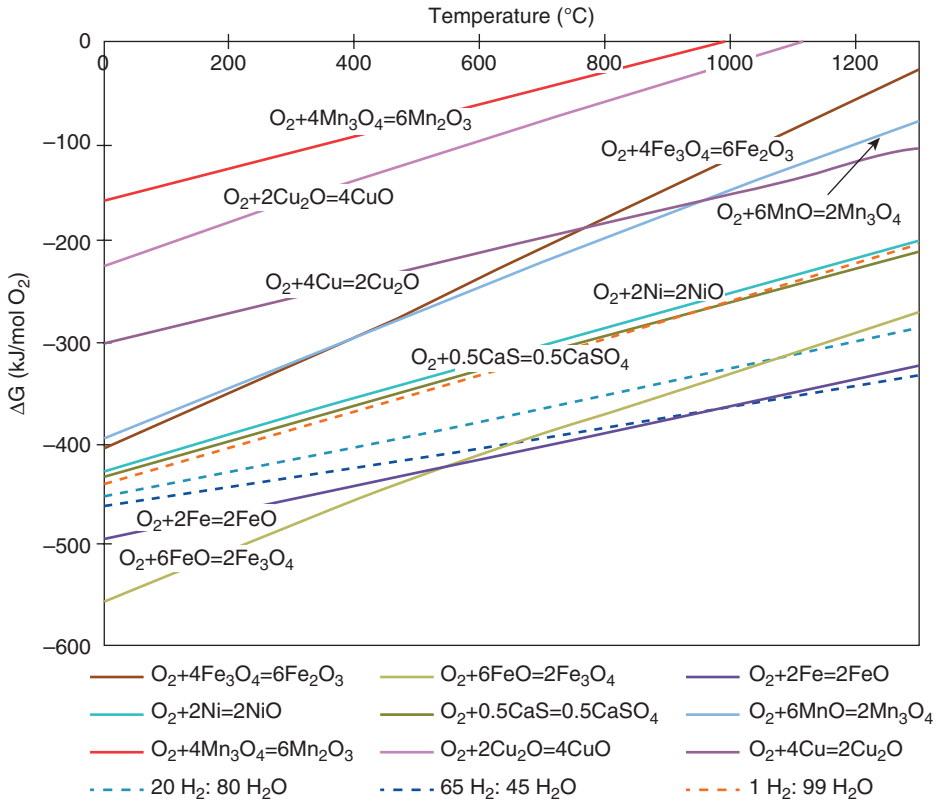

FIGURE 9 | Ellingham diagram for metal oxides used in chemical looping schemes.

if its operating line is above the fuel line. In the case 99% conversion of CO to CO_2 is desired, Mn, Cu, and Fe are capable of achieving this purity of CO_2 based on this thermodynamic model. However, Ni and $CuSO_4$ based oxygen carriers are limited from achieving greater than 99.5% purity CO_2. Ni-based oxygen carriers have been heavily studied for CLC processes due to their favorable kinetics and potential catalytic effects for enhanced fuel conversion. However, growing concerns over the cost, health, and environmental impacts of using Ni-based oxygen carriers have shifted many researchers to consider more inexpensive and benign metal oxides such as Fe. In case of $CaSO_4$, recyclability studies shows the oxygen carrier reactivity decreases with increased cycles due to the loss of sulfur and the formation of CaO.[47]

The conversion of Cu- and Mn-based oxygen carrier with fuel is highly spontaneous due to its tendency to form molecular oxygen in an oxygen-depleted environment as described in *Chemistry* section. This high oxygen carrier reducibility poses a challenge for its regeneration in the combustor reactor. For the oxygen oxidation, from Figure 9, the Gibbs free energy for the metal oxide oxidation with 1 mole of O_2 must be less than the Gibbs free energy for the partial pressure of O_2 considered. In the case of atmospheric air, the Gibbs free energy for net reaction of Mn and Cu-based oxygen carriers with air is approaches zero with increasing operation temperature. This result indicates potential kinetic limitations with these oxygen carriers, which would result in greater residence time requirements for the combustor reactor operation compared to non-CLOU oxygen carriers. Additionally, the reduction of Cu-based oxygen carriers in the reducer must be carefully limited to Cu_2O as reducing the metal oxide to metal copper may result in oxygen carrier agglomeration due its low melting point.

Support materials are commonly used to enhance the particle performance and/or resistance to attrition. Purely inert support materials are used only to enhance the particle strength while remaining unreactive throughout the cycle redox reaction. The support materials include spinel structures of aluminates such as $MgAl_2O_4$ and $FeAl_2O_4$ and clays such as bentonite and kaolin that are highly unreactive with the primary metal oxide.[48] The inert support material may also assist in raising the melting temperature of the pure metal oxide. Whitty et al. reported that using SiC/SiO support on Cu-based oxygen carrier prevented bed agglomeration in a fluidized bed operated at up to 1000 °C.[49] Other support materials

can enhance the reactivity of the metal oxide. Fan et al. reports metal oxide supports such as CeO_2 can enhance the ionic diffusion of atomic oxygen into and out of the oxygen carrier while preventing the migration of the metal cation.[27] In case of CLC for solid fuel conversion, support metals such as K, Na, and Li can be used to enhance coal gasification due to the catalytic properties of these materials.

Natural occurring ores and minerals such as limestone, ilmenite, and iron ore have also been extensively studied. The use of natural ores and minerals in CLC processes eliminate the particle make-up costs associated with oxygen carrier synthesis. However, natural occurring minerals generally have a lower reactivity and potentially a higher attrition rate than synthesized particles. Synthesized particles may have a higher particle cost, but lower make-up rate while naturally occurring ores and mineral may have the reverse. Large-scale demonstration systems are under development to study both synthesized and naturally occurring oxygen carriers. *Performance Results* section summarizes the findings from several of these CLC units.

Performance Results

It is estimated that there are 24 CLC systems that have operated for thousands of hours in total, and they all have the same goal of confirming the feasibility of CLC as an economical power generation technology with carbon capture. In this section, performance results from these units are described both quantitatively and qualitatively.

Gaseous Fuels

Various studies were performed in the 10-kW_{th} unit developed by Lyngfelt et al. Initially, freeze-granulated nickel oxide was used to study gaseous fuel conversion for 100 h.[32] The reducer gas contained minimal CO, H_2, and CH_4, and a fuel conversion of 99.5% was achieved. When Fe_2O_3 was used, the CO and CH_4 concentrations ranged between 2 and 8%. Redox cycle tests indicated the oxygen carrier reactivity could be maintained. However, investigation of NiO particles revealed incomplete oxidation of the oxygen carriers exiting the combustor was occurring.[50] Linderholm et al. were able to subject spray-dried $NiO/NiAl_2O_4$ material to cyclic natural gas and air conditions for 1000 h in a 10-kW_{th} unit, with the purpose of determining the long-term reactivity and attrition of the oxygen carrier.[51] The temperature of the reducer ranged from 800 to 950 °C. Natural gas conversion was high with combustion efficiencies above 90%. With over 400 h of testing, Linderholm et al. showed the CH_4 conversion can be increased from 95–98 to 99% with the addition of Mg-based oxygen carrier, increasing the combustion efficiency to greater than 90%. Agglomeration attributed to poor mixing was observed, and downtime to open the vessel and clear blockages was required. The CLOU perovskite oxygen carrier $CaMnO_3$ produced from low-cost materials was also studied in the 10-kW_{th} unit with promising results, such as high oxygen release and high methane conversion.[52] The material however suffered from high attrition, but this fact could be countered by the low material cost. A similar perovskite structure, $CaMn_{0.9}Mg_{0.1}O_3$ shows similarly promising results, yet the material was more resistant to attrition.[53]

Ryu et al. demonstrated a 50-kW_{th} unit using NiO and CoO to achieve methane conversions around 98%.[38] Son and Kim performed methane conversion studies with NiO as the main oxygen carrier supported with Fe_2O_3/bentonite in their DCFB system.[37] The reducer was operated between 650 and 950 °C. For their system, increasing the NiO content of the oxygen carrier increased the methane conversion, as NiO has more favorable kinetics.

Kolbitsch et al. initially converted natural gas in a 140-kW_{th} unit, with reducer temperatures between 775 and 950 °C, using NiO with $NiAl_2O_4$ and $MgAl_2O_4$ as support material. Methane conversions were above 92%, with the highest conversions occurring with $MgAl_2O_4$ support and a high reducer temperature. However, the unit had difficulty fully oxidizing the oxygen carrier in the combustor.[54] Later tests in the same pilot unit used ilmenite[31] as well as naturally occurring olivine ($(Fe,Mg)_2SiO_4$).[55]

Solid Fuels

For the 10-kW_{th} solid-fuel unit developed by Lyngfelt et al., initial demonstrations involved conversion of petroleum coke and a South-African coal as the fuel with ilmenite as the oxygen carrier. The reducer and oxidizer operating temperatures were 950 and 1000 °C, respectively.[56,57] A total of 22 h was tested with South African coal. At lower gas velocities, the oxygen carrier exhibited agglomeration. Around 18 h of stable operation were achieved with petroleum coke. For both studies, the solid–fuel conversions ranged from 50 to 80%, which was due to poor performance of the reducer cyclone. In addition, the conversion to CO_2 ranged from 27 to 36% and 78 to 81% for the coke and coal studies, respectively, and the CO and CH_4 concentrations were around 3 and 1 vol%, respectively. This was attributed to the coal volatiles and gasified products bypassing the oxygen carrier. As a result of the low carbon stripper

recovery efficiency and solids residence time, CO_2 capture between 82 and 96% was achieved.

These results were used to improve the design for future experiments. Moving the solid fuel injection below the surface of the bed increased the gas conversion.[39] However, mass transfer limitations still existed, and because of the small size of the fluidized bed, slugging occurred, which acts to 'short circuit' the gases through the bed. A further modification included pretreating the caking coals to prevent fuel agglomeration. Other oxygen carriers tested in this unit included a manganese ore,[39] ilmenite ore with lime, and manganese ore with lime mixtures.[58] The manganese ore increased the gasification rate by about four times and increased the carbon capture efficiency and gas conversion. It was noted that the addition of lime to manganese ores in the conversion of petroleum coke increased the performance.[58]

The design of the 100-kW_{th} unit developed by Lyngfelt et al. was tested using a cold flow model for operability studies.[59,60] The main oxygen carrier tested in the hot unit was ilmenite, and the fuels tested in this unit included Mexican petroleum coke[41] and Columbian bituminous coal.[61] For runs with Mexican petroleum coke, the oxygen demand was lower because the coke contains minimal volatiles.[60] For bituminous coal, the carbon capture efficiency and oxygen demand ranged from 96.4 to 99.5% and 16.3 to 21.6%, respectively, during the five reported trials.

The 10-kW_{th} system, operating in a temperature range of 740–920 °C in the reducer, developed by Shen et al. used iron oxide as the oxygen carrier and was operated for over 30 h. With biomass as the fuel, a carbon dioxide conversion of 53.7–65.1% was achieved.[62] The authors observed lower conversions at higher temperatures, as the oxygen carrier cannot fully convert the biomass due to thermodynamic limitations. Further studies included understanding the rate of reaction deterioration with time over 100 h using NiO/Al_2O_3. Deterioration in reactivity was attributed to surface sintering of the particle. The effect of ash deposition on the particle was determined to be minimal as measured by XRD spectra, most likely due to attrition in the fast fluidized bed combustor.

The smaller 1-kW_{th} unit incorporated design changes in the loop-seal configuration. Part of the CO_2 capture losses observed in the 10-kW_{th} system was due to gas bypassing from the reducer to the combustor.[63] The loop seal became external to the reducer and was now fluidized by steam. After these changes, further parametric studies on the 1-kW_{th} unit were performed, showing the change in performance with an Australian iron ore with biomass and coal.[64] Runs using biomass also studied the effects of mineral alkali on the oxygen carrier; XRD and EDX showed that potassium coated the particle. Further studies were performed with co-precipitated NiO/Al_2O_3 particle and coal for 30 h of operation at a reducer temperature of 970 °C and combustor temperature of 1020 °C.[65] The fate of sulfur species in the reducer (SO_2, H_2S, and COS) and the combustor (SO_2) were studied and interpreted based on reaction equilibrium of nickel compounds and potential homogeneous reactions.

To enhance solid fuel gasification, Gu et al. studied dolomite-modified and cement/dolomite-modified iron ore in the 1-kW_{th} unit.[66] While effective below 930 °C, the dolomite-modified ore began to sinter at higher temperatures, but addition of cement allowed for the formation of $Ca_2Si_2AlO_7$ which prevents sintering. Niu et al. also converted dewatered sludge using hematite ore as an oxygen carrier.[67] The fate of phosphorus was studied, which is a highly concentrated element in waste sludge. The resulting phosphorus from CLC conversion of sludge was water soluble, in the form of $CaHPO_4$ and $CaH_2P_2O_7$, as opposed to $Ca_3(PO_4)_2$ and $AlPO_4$ which is normally found in sludge incineration.

In the 1.5-kW_{th} unit developed by Abad et al., one of the oxygen carriers used for testing was copper oxide supported with the spinel $MgAl_2O_4$ for use as a CLOU particle.[68] The carbon capture efficiency was nearly 100%, and the rate of char conversion at 960 °C demonstrated advantages of CLOU over traditional CLC processes. Abad et al. noted that with bituminous coal used in the test (El Cerrejon), a residence time of 300 s was required to achieve a char conversion of about 97%.[40] Different solid fuel particle size ranges were also studied with ilmenite over a temperature range of 870–950 °C.[69] The fuel particle size had an effect on the oxygen demand and combustion efficiency, but not on the carbon-capture efficiency or char conversion. The char conversion ranged from 15% at 870 °C to 82% at 950 °C, while the carbon capture efficiency ranged from 35% at 870 °C to 86% at 950 °C. Further studies included fate of sulfur using lignite coal and 60% CuO and $MgAl_2O_4$ support at temperatures around 930 °C.[68] They were able to achieve a carbon capture efficiency of 97.6% at 935 °C operating temperature with 87.9% of the sulfur exiting the reducer flue gas stream as SO_2.

The 1-MW_{th} unit developed by Epple et al. has been commissioned and operated for 480 h. Autothermal operation was achieved, but a high solids circulation rate was required for operation. The oxygen demand was around 20% using ilmenite.[70]

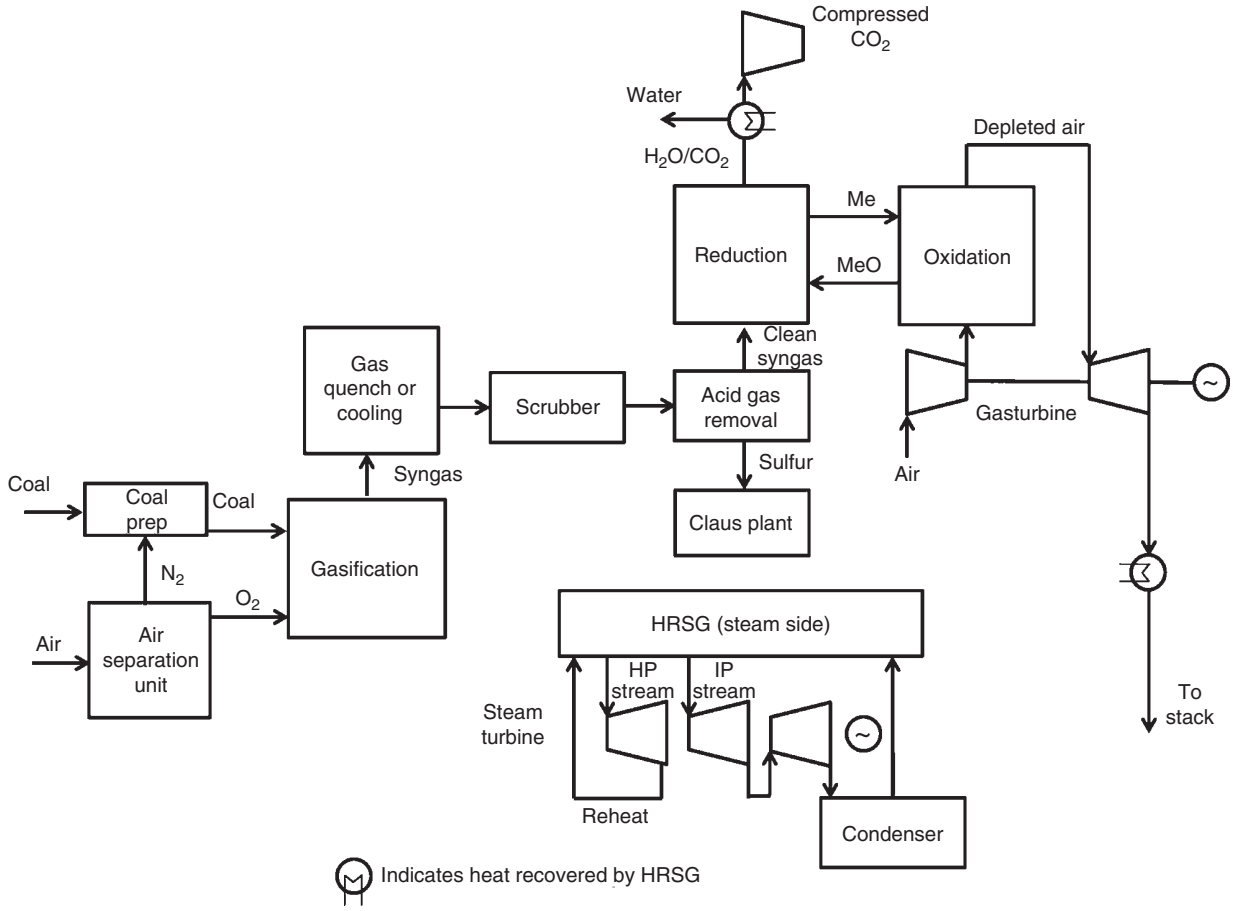

FIGURE 10 | Chemical looping combustion used for syngas combustion in IGCC.

Fan et al. have operated a 25-kW_{th} unit with metallurgical coke, lignite, sub-bituminous, bituminous coal, and wood pellet-based biomass,[45,46,71,72] The studies were performed for over 680 h of operation achieving nearly complete volatile and char conversions to CO_2 and steam. The 25-kW_{th} unit represents the first fully integrated CLC demonstration for solid fuel conversion with a moving bed reducer. A 200-h demonstration confirmed the smooth operability of the system design with no solid circulation or gas flow issues observed. Steady-state carbon conversions ranged from 90 to 99% with an average of 97.9%. The CO_2 purity was around 99.7%, while average CO and CH_4 concentrations were around 0.20 and 0.10%, respectively, confirming the moving bed operation capability for nearly full solid fuel conversion to CO_2.

Advanced Configurations and Process Simulation for Power Production

In advanced configuration of the CLC process, a number of authors have considered replacing the combustion of hydrogen/syngas in an integrated gasification combined cycle (IGCC) system with CLC to improve the process efficiency with carbon capture. A process diagram of IGCC with CLC is shown in Figure 10. Syngas is converted to CO_2 in the reducer, while the combustor in the CLC system would receive air from the compression stage of the Brayton cycle, exothermically regenerate the oxygen carrier, and exhaust the hot spent air through a gas turbine. The CLC system would effectively replace the water–gas shift reactor and the CO_2-absorption unit, and it would reduce the requirements of the acid gas removal system. Erlach et al. determined in their analysis that a CLC/IGCC plant has a 3% efficiency increase with lower CO_2 emissions (7 kg/MWh_{el} compared to 125 kg/MWh_{el}) than compared to traditional IGCC with precombustion carbon capture.[73] Other authors have considered using two CLC systems at different temperatures and pressures for oxygen carriers that produce slightly exothermic reactions in the reducer.[74] Natural gas combined cycle (NGCC) has also been considered with CLC.[75]

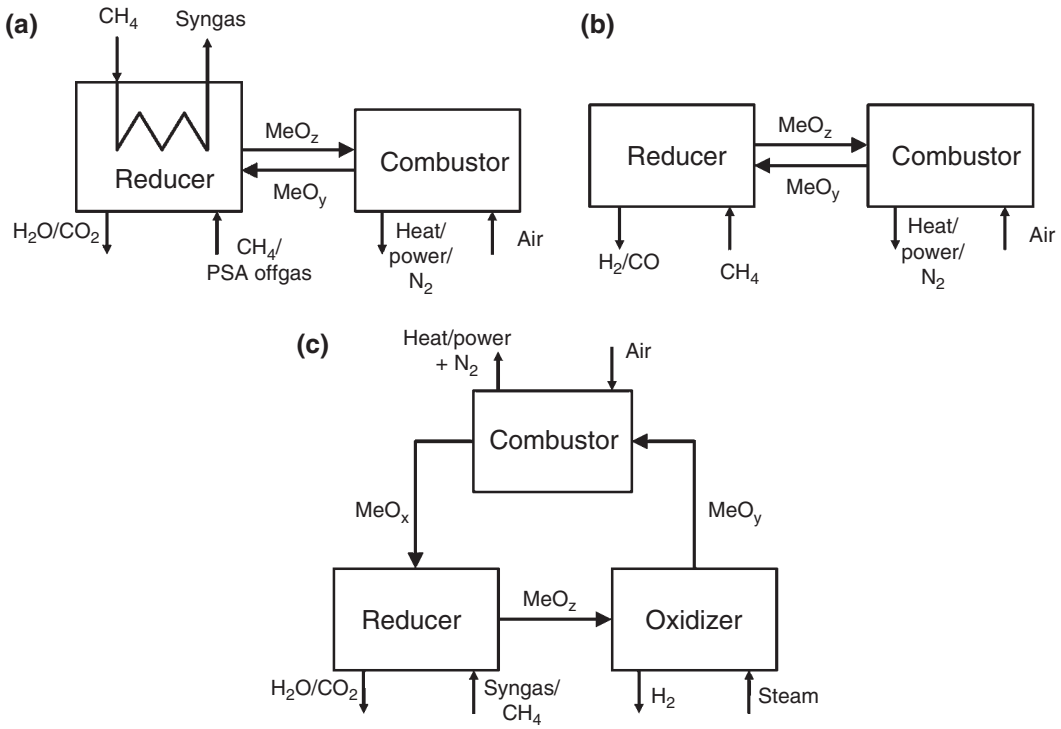

FIGURE 11 | Chemical looping schemes for production of chemicals from methane: (a) chemical looping reforming (CLR); (b) chemical looping partial oxidation (CLPO); and (c) syngas chemical looping.

An advanced CLC system analyzed by Xiang et al. consists of a pressurized-pipe coal slurry gasification system that receives energy from the combustor.[76] Assuming equilibrium conditions occur for steam gasification of the coal as well as for the reducer and combustor with nickel oxide as the carrier, the system net efficiency ranges from 43 to 45.5% (LHV) with a carbon capture range of between 85 and 98%.

CHEMICAL LOOPING FOR HYDROGEN OR SYNGAS PRODUCTION WITH CARBON CAPTURE

While traditional steam methane reforming (SMR) is well established in industry, carbon capture is difficult, as the partial pressure of the CO_2 from the furnace providing energy for the reformer is low.[77] Chemical looping can serve as an efficient means for hydrogen and syngas generation with inherent CO_2 capture capabilities. The present section reviews the reaction scheme for these chemical looping systems and summarizes the reaction scheme, process design concept, performance and simulation results to date.

Chemistry Scheme

Figure 11 describes three methods that a chemical looping scheme can produce hydrogen or syngas from a carbonaceous feedstock while efficiently capturing carbon.

The first method, shown in Figure 11(a), is called chemical looping reforming (CLR), proposed by Ryden and Lyngfelt.[78] The process is akin to a conventional SMR process, in that methane and steam react in catalyst-filled tubes to produce synthesis gas. A CLC system replaces an external furnace that normally provides energy to the endothermic reforming reaction in the tubes. The catalyst tubes reside in the reducer, which receives hot particles from the combustor. Fuel and off-gas from a pressure swing adsorption (PSA) unit are fed into the reducer. For hydrogen production, a water–gas shift reactor is used for shifting the CO in the syngas to CO_2. An advantage of the system is that carbon is captured from the reducer, and the off-gas from the PSA unit can be reused as a fuel for the reducer. The disadvantage of the system is that a water–gas shift reactor and PSA are still required, reducing the overall process efficiency. To date, no integrated CLC with SMR systems of this design have been studied.

Shown in Figure 11(b), chemical looping partial oxidation (CLPO) allows for partial oxidation of the fuel using the chemical looping concept. Conventionally, partial oxidation implies that only oxygen is used, while autothermal reforming uses both steam

and oxygen. The reactions used in CLPO chemical looping are similar to conventional reforming and partial oxidation, except the metal oxide provides oxygen to the fuel.

$$CH_{4(g)} + MO_{n(s)} = CO_{(g)} + H_{2(g)} + MO_{m(s)}. \quad (7)$$

When the metal oxide becomes sufficiently reduced, the metal can catalyze the SMR reaction. Regeneration occurs in the combustor. The CLPO chemical looping scheme eliminates the need for an air-separation step for producing high-quality syngas.

The third method uses reduced metals that produce hydrogen when reacted with steam. An intermediate oxidation reactor after the reducer, as shown in Figure 11(c), undergoes the following reaction.

$$MO_{x(s)} + H_2O_{(g)} = MO_{y(s)} + H_{2(g)}. \quad (8)$$

A limited number of metals can be oxidized by steam. As demonstrated in the Lane process, the one most commonly studied in chemical looping for hydrogen production is iron.

$$3\,Fe_{(s)} + 4\,H_2O_{(g)} = Fe_3O_{4(s)} + 4\,H_{2(g)}. \quad (9)$$

$$FeO_{(s)} + H_2O_{(g)} = Fe_3O_{4(s)} + H_{2(g)}. \quad (10)$$

The reaction, which is slightly exothermic, produces magnetite (Fe_3O_4) by reacting steam with iron in what is known as the steam-iron reaction. Processes that use this chemistry include the syngas chemical looping (SCL) process developed by Fan et al.[79] the iron-based IGCC configuration conceived by Cormos,[80] the one-step decarbonization process proposed by Mizia et al.,[81] and the three-reactor scheme proposed by Kang et al.[82] The production of hydrogen using steam to oxidize the reduced iron and solar energy to reduce the iron has also been proposed by Nakamura.[83] In some processes, such as the SCL process, the iron oxide regenerated from steam can be further oxidized in a combustor to produce energy for electricity or steam generation.[26]

Reactor Design

Overall, the reactor design requirements for hydrogen or syngas generation from a chemical looping scheme are similar to that for chemical looping combustion described previously, in that the reactor hydrodynamics, gas sealing, particle attrition, and solids handling need to be taken into account. Additional considerations include the fuel gas and oxygen carrier contact and thermodynamic conversion limitations.

Pure hydrogen generation in an intermediate oxidizer such as in Figure 11(c) has mainly been considered for iron, but other schemes have been proposed with cobalt and nickel coupled with iron.[84] For iron oxide, the reducer needs to convert the oxygen carrier below Fe_3O_4. As the reduction of Fe_3O_4 and FeO for many fuels is less exergonic than for Fe_2O_3, there is an issue in terms of the purity of the CO_2 produced from the reducer flue gas stream; this is discussed in detail in the studies by Li et al.,[72] Fan,[26] and Svobota et al.[85] The limitation can be overcome by using a Mode II design as iron can be reduced to Fe/FeO while maintaining full fuel conversion as explained in *Reactor Design for Power Production* section. Xue et al. have suggested using a bubbling fluidized bed of highly reduced particle coupled with a fast fluidized bed riser of fresh Fe_2O_3.[86] The SCL process developed by Fan et al. uses the Mode II reducer configuration to fully oxidize the fuel while reducing the oxygen carrier to a mixture of Fe and FeO. The high oxygen carrier conversion allows the oxidizer to generate hydrogen from Reactions 9 and 10.

For syngas generation, the designs by Proll et al., Lyngfelt et al., and Abad et al. discussed in *Chemical Looping for Power Production with CO_2 Capture* section can also produce syngas by reducing the oxygen carrier to fuel flow ratio in the reducer. The unit by Proll et al. is designed for gaseous fuel conversion, while those by Lyngfelt et al. and Abad et al. can use either gas or solid fuels. Nickel oxides have been proposed as oxygen carriers for CLPO chemical looping as the reduced metal promotes the steam-methane reforming reaction.[87] Many of the CLPO chemical looping systems use fluidized bed reducers. However, the disadvantage of fluidized reducers for syngas generation is the diluted quality of the syngas, as CO_2 is prominent in the product gas stream. Mixing in a fluidized bed prevents control of the oxygen carrier reduction and syngas quality. On the other hand, introducing natural gas co-current to the flow of oxygen carrier in a packed moving bed allows for better control of the oxygen carrier and fuel conversion. At the methane inlet, concentrated methane only reacts with fresh oxygen carrier, which is unlikely to catalyze methane decomposition; at the reducer outlet, the reduced oxygen carrier provides a minimal amount of oxygen to convert the remaining methane into syngas without producing more CO_2.

Oxygen Carrier Development

The oxygen carrier used for these chemical looping systems differ between the three methods for syngas and hydrogen production. For the first method,

the CLR process, the chemical looping scheme is consistent the CLC process for power generation. Therefore, the oxygen carrier development described in *Oxygen Carrier Development* section is applicable to this method of syngas generation.

For CLPO chemical looping process, the primary metal oxides considered are Ce, Fe, and Ni. Fan et al. performed a thermodynamic analysis of each metal oxide to determine the optimum conditions for high purity syngas production. The results show that in order to produce >90% syngas purity with Ni- and Fe-based oxygen carriers, both metal oxides had to be reduced to their metallic states making the process highly susceptible to carbon deposition and carbide formation. Ce-based oxygen carrier showed favorable thermodynamics to produce syngas without carbon deposition. However, experimental results showed the slow reaction kinetics of CeO-Ce_2O_3 limited the methane conversion capability of this metal oxide. Due to the limitation of single metal oxides, binary metal oxides were also considered to enhance the selectivity of the oxygen carrier for syngas production. Iron-titanium metal oxide (ITCMO) was determined as the optimum oxygen carrier for CLPO chemical looping process. Thermodynamic simulations and experimental results prove the CLPO chemical looping process with ITCMO oxygen carriers is capable of producing >90% purity syngas at nearly a 2:1 H_2:CO ratio.[88]

For the third method, chemical looping schemes used for CO_2 capture and hydrogen co-generation use a water-splitting steam reaction described in *Chemistry Scheme* section. The metal oxides considered for this type of system are consistent with CLC processes. From Figure 9, the Gibbs free energy for the reverse water splitting reaction at different concentrations of H_2 and H_2O are provided. In order for a metal oxide to perform the water splitting reaction, it must have a Gibbs free energy less than the reverse water splitting reaction at a given temperature. The only oxygen carrier capable of this is iron in the Fe/FeO oxidation state. Reducing Fe_2O_3 to FeO/Fe in a Mode I reducer reactor would result in complete fuel conversions. A Mode II reactor operation would be the optimum choice to ensure complete fuel conversion from the reducer reactor and the ability to generate hydrogen from the steam-iron reaction in a separation oxidizer reactor. The support materials used for these oxygen carriers to enhance reactivity and strength are consistent with those described in *Oxygen Carrier Development* section. *Performance Results* section summarizes the demonstration results for chemical looping systems for syngas and hydrogen generation.

Performance Results

For pure hydrogen generation, numerous kinetic studies have been performed with various oxygen carriers.[89–92] Laboratory or pilot scale units have already either been developed or are in the process of development. Hacker et al. have proposed an iron-based 10-MW_{th} syngas-to-hydrogen process using a total of seven fixed beds of iron integrated with a solid-oxide fuel cell.[93,94] The process consists of cycling the seven fixed beds between reduction with syngas, oxidation with steam, and purge with nitrogen. Xue et al. have proposed a compact fluidized bed and developed an integrated, scaled cold-flow model of the process.[86]

For the SCL system developed by Fan et al., over 360 h of operation have been completed in a 25-kW_{th} sub-pilot experimental unit.[95] The continuous operations resulted in nearly 100% syngas conversions and >99.99% purity hydrogen production.[79] The successful operation of the sub-pilot unit confirms that the Mode-II moving bed operation is capable of high fuel conversion and high purity hydrogen production. A pilot-scale SCL test unit was constructed in Wilsonville, AL, USA. This pressurized test unit will operate with syngas produced from a transport gasifier. The pilot-scale SCL unit consists of no mechanical moving parts in the system. A 1:1 scale cold flow model was also constructed and tested with over 200 h of successful operation. The Mode-II reducer operation was also studied for the conversion of methane in the sub-pilot SCL unit.[96] Multiple sensitivity studies were conducted by varying the oxygen carrier and methane flow rate to determine the optimum operating conditions. The results indicated the moving bed process can fully convert the methane to CO_2 while enhancing the oxygen carrier conversion to Fe/FeO for subsequent hydrogen production from the oxidizer.

Initial experimental attempts at syngas generation from methane were performed by Lewis and colleagues using copper oxide deposited on silica gel in a 1.2-m tall fluidized bed reactor.[97] Methane reforming was performed with steam as well as carbon dioxide at temperatures between 630 and 919 °C. The process was not integrated with a combustor reactor, but the results were obtained to determine the feasibility of the methane decomposition reaction to produce syngas as well as its kinetics. Methane decomposition was determined to be reaction rate limited instead of gaseous diffusion limited, and the two-step mechanism proposed for syngas generation involved (1) rapid and full oxidation of the methane to CO_2 and H_2O, and (2) rate-limiting reforming of the remaining methane with CO_2 and H_2O to form CO and H_2. A variety of supports such as silica, magnesia, and

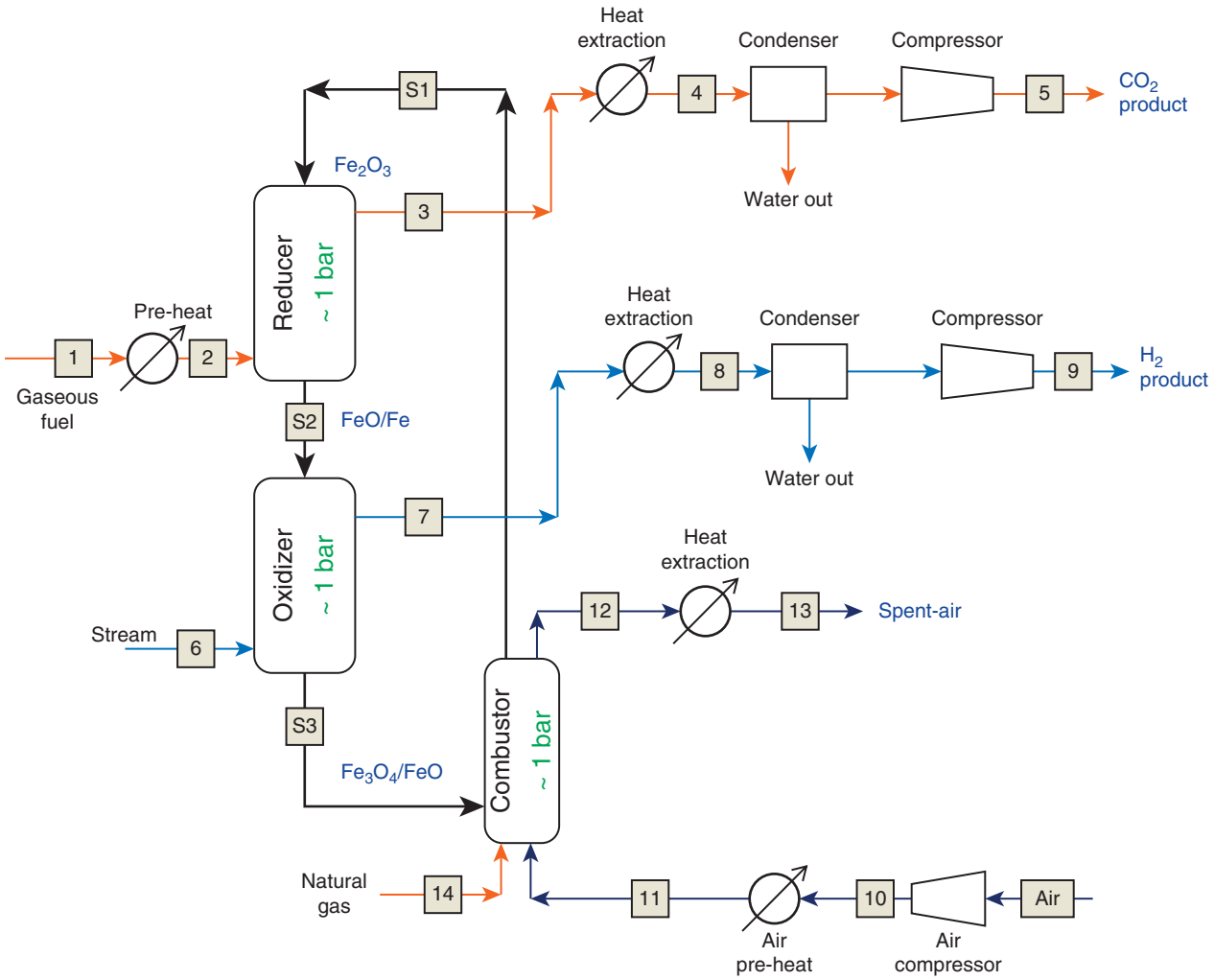

FIGURE 12 | Layout of the syngas chemical looping concept.

alumina were tested with copper, with the highest conversion of methane decomposition and syngas selectivity (90 and 95%, respectively) occurring with mixture of silica-supported CuO and silica-supported NiO.

Ryden et al. were able to perform CLPO with methane and steam to produce syngas in a small 300-W_{th} unit using NiO/$MgAl_2O_4$ as oxygen carrier.[98] The amount of stoichiometric oxygen provided to the methane was in the range of 0.4–0.5 in the temperature range of 820–930 °C, and both dry reforming and steam reforming (with 25 vol% water added to the methane fuel feed) were performed on the oxygen carrier to observe if SMR would occur on the reduced nickel. The oxygen carrier experienced extensive carbon deposition without steam injection, but the reactivity was maintained over 41 h.

Proll et al. performed extensive syngas generation studies using a nickel-based oxygen carrier. The reducer was operated at 747–903 °C, with air-to-fuel ratios from 0.4 to 1.1.[99] At the lowest ratio, the syngas composition was 20% CO, 38% H_2, 10% CO_2, and 32% H_2O. Work was performed by de Diego et al. in a 900-W_{th}, with reducer operating temperatures ranging from 800 to 900 °C, using NiO supported with alumina, and NiO/CH_4 ratios ranging from 1 to 8.[100] Different steam-to-methane ratios were studied up to a ratio of 0.5. At a steam-to-methane ratio of 0.3 and a NiO/CH_4 ratio of 1.8, the syngas composition was around 60–65 vol% H_2, 22–25 vol% CO, 5–10% steam, 4-8% CO_2, and less than 1% methane.

Fan et al. developed a CLPO process called the shale gas to syngas (STS) chemical looping process using a co-current packed bed configuration with iron oxide and demonstrated the process in sub-pilot scale unit.[88] Experiments were conducted with atomic oxygen to methane ratios at 2.2 and 2.8 were used. At temperatures of 975 and 900 °C, high syngas selectivity (>85%) and a H_2/CO ratio near 2 with

TABLE 2 | Reducer Conditions for the Syngas Chemical Looping Process

Stream No.	1	2	3	4	5	S1	S2
Temperature (°C)	38	530	1200.9	148.9	95.9	1190	802.3
Pressure (bar)	30	30	1.01	0.98	152.72	10	1.01
Gas mole flows (kmol/h)							
CO			0.02	0.02	0.02		
CO_2	2.543	2.543	205.881	203.823	203.817		
CH_4	183.626	183.626	trace	trace			
C_2H_6	6.249	6.249	trace	trace			
C_3H_8	1.36	1.36	trace	trace			
C_4H_{10}	0.789	0.789	trace	trace			
H_2			0.015	0.015	0.015		
H_2O			395.367	391.413	0.302		
N_2	2.563	2.563	2.561	2.535	2.535		
NO			0.004	0.004	0.004		
O_2			0.68	0.673	0.673		
Mass flow (kg/h)	3423.29	3423.29	16277.65	16277.65	9068.669	170190.1	157335.7
Solids mole flow (kmol/h)							
Fe							402.331
$FE_{0.947}O$							475.458
Fe_3O_4							
Fe_2O_3						426.295	
Inert						1001.498	1001.498

TABLE 3 | Oxidizer Conditions for the Syngas Chemical Looping Process

Stream No.	6	7	8	9	S3
Temperature (°C)	200	803.7	148.9	20.6	764.8
Pressure (bar)	1.31	1.01	1.01	21.72	1.01
Gas mole flows (kmol/h)					
CO					
CO_2					
CH_4					
C_2H_6					
C_3H_8					
C_4H_{10}					
H_2		487.806	487.806	487.806	
H_2O	736.584	248.77	404.77	0.462	
N_2					
NO					
O_2					
Mass flow (kg/h)	13269.76	5465.023	8275.407	991.679	165141.1
Solids mole flows (kmol/h)					
Fe					
$Fe_{0.947}O$					660.443
Fe_3O_4					75.717
Fe_2O_3					
Inert					1001.498

almost 100% methane conversion was produced, showing the viability of using a co-current moving bed of oxygen carriers for syngas generation.

Simulation Results and Advanced Configurations

A number of authors have performed the mass and energy balances of a chemical looping system producing hydrogen or syngas. For example, Chiesa et al. have analyzed a three-reactor system for hydrogen production from methane and carbon capture.[101] Similarly, a detailed analysis is performed by the authors to analyze the feasibility of utilizing a Mode II chemical looping system for hydrogen production from natural gas. The methodology is outlined in Figure 12. The overall material balance for a 50 MW_{th} natural-gas processing unit is shown in Tables 2–4. The chemical looping system produces excess heat, which can be used for satisfying the parasitic energy requirements. The solids enter the reducer at 1190 °C and exit at 800 °C, and the natural gas inlet stream is preheated to 550 °C. A convection pass extracts heat from the CO_2 outlet stream, and energy is also extracted to preheat the methane. A condenser removes the water before sending this stream to a CO_2 compressor, which pressurizes the CO_2 stream to 152 bar. The product stream exiting the oxidizer goes through a heat-extraction step before passing through condensers to separate unconverted steam. With a carbon capture of 93.91%, the system has a cold-gas efficiency of 76.81%, compared to 72.18% for conventional SMR.[102] For the baseline SMR process, external electricity purchase is required.

An iron-based chemical looping system for liquids production was designed to produce 50,000 barrels per day of liquid fuel as shown in Figure 13. The Fischer-Tropsch and refining complex were modeled to utilize syngas and produce gasoline.[102,103] The reducer was modeled using four equilibrium stages, with co-current flow of methane and iron oxide to produce syngas for Fischer-Tropsch synthesis. Heat is extracted from the combustor to generate electricity, which is used to offset parasitic energy requirements. The H_2 production plant also uses an iron-based chemical looping system to increase the natural gas utilization efficiency as compared to the steam methane system used in the baseline case.[104–106] Process results are shown in Table 5, which compares the chemical looping syngas generation system to both a conventional autothermal and steam reforming unit. The chemical looping system uses a lower amount of steam per mole of carbon processed when compared to the conventional system. Another advantage is the oxygen comes from the iron oxide as opposed to an air separation unit (ASU). This results in a higher selectivity in natural gas oxidation. It can be seen that for an equivalent syngas specification (H_2/CO ratio), the chemical looping system has higher selectivity.

The higher efficiency of syngas production means less natural gas is consumed for the same output of syngas. The baseline carbon-utilization value is

TABLE 4 | Combustor Conditions for Syngas Chemical Looping Process

Stream No.	AIR	10	11	12	13	14
Temperature (°C)	15	31.9	600.3	1193.8	148.9	38
Pressure (bar)	1.01	1.18	1.18	0.91	0.85	30
Gas mole flows (kmol/h)						
CO				<0.001	<0.001	
CO_2	0.353	0.353	0.353	14.946	14.946	0.155
CH_4						11.178
C_2H_6						0.38
C_3H_8						0.083
C_4H_{10}						0.048
H_2				<0.001	<0.001	
H_2O	11.665	11.665	11.665	39.687	39.687	
N_2	911.045	911.045	911.045	910.895	910.895	0.156
NO				0.661	0.661	
O_2	244.375	244.375	244.375	61.849	61.849	
AR	10.84	10.84	10.84	10.84	10.84	
Mass flow (kg/h)	34000	34000	34000	29325.56	29322.16	208.388

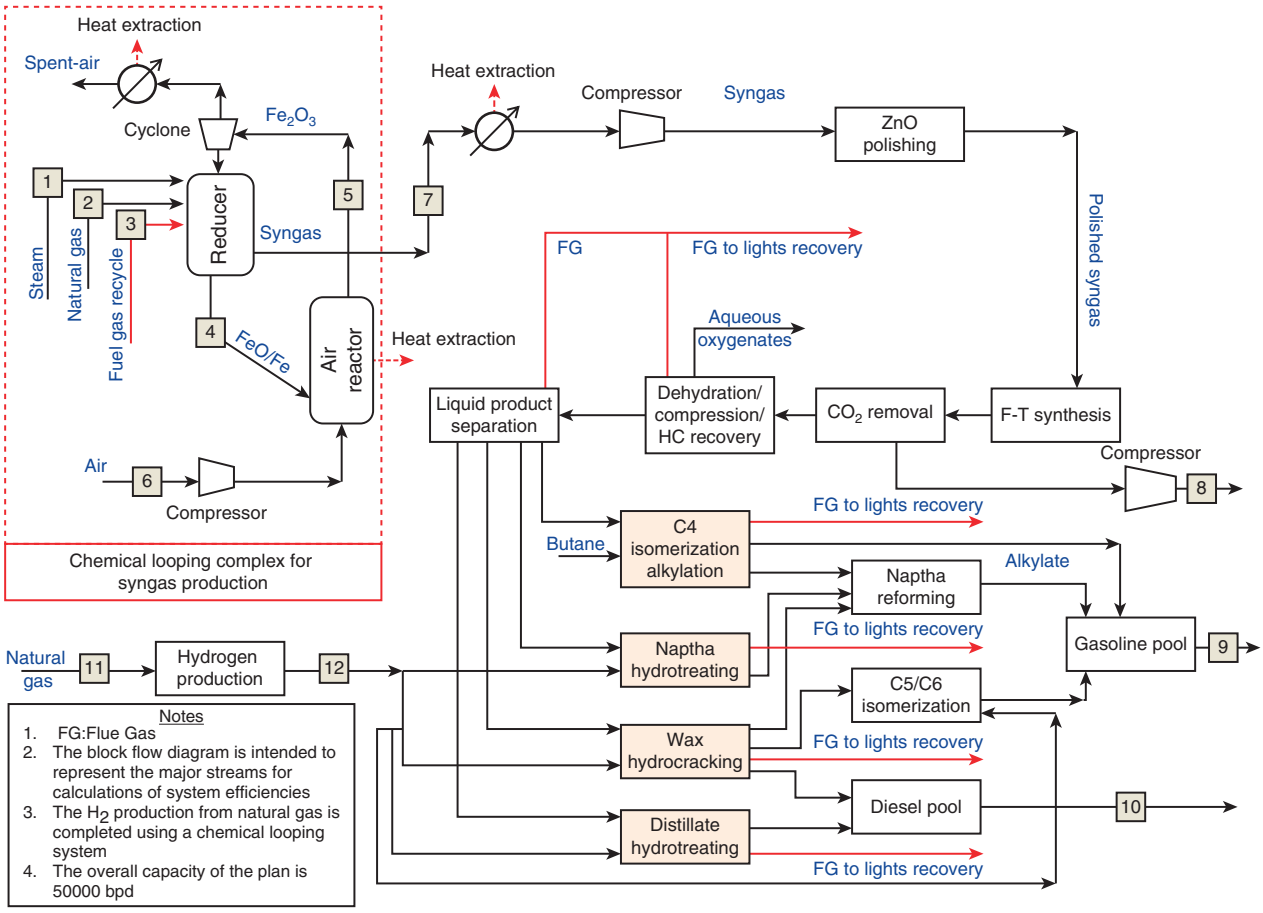

FIGURE 13 | Process configuration for syngas generation from methane for liquid fuels production from Fischer-Tropsch.

TABLE 5 | Carbon Efficiency and Overall Production for the Chemical Looping Case and the Base-Line DOE Case

Process Comparison		
Component	Base Case	Chemical Looping
H_2O/C (–)	0.68	0.2
H_2/CO (–)	2.19	2.18
Stoichiometric number (–)	1.59	1.84
Nat gas feed flow (kg/h)	354,365	334,427
Butane feed flow (kg/h)	18,843	18,843
Diesel fuel (bbl/day)	34,543	34,543
Gasoline (bbl/day)	15,460	15,460
Total liquids (bbl/day)	50,003	50,003
Carbon efficiency		
Natural gas to liquid fuels	81.80%	86.68%

81.8%, while a chemical looping system is 86.68%, as shown in Table 5. When the heat produced is used to generate electricity, it is adequate to offset system parasitic energy demands. The higher intrinsic selectivity coupled with lower steam consumption and no molecular oxygen requirement makes chemical looping a promising, economical alternative to conventional systems.

CONCLUSIONS

The chemical looping concept has been demonstrated worldwide using a variety of oxygen carriers, fuel feedstocks, and reactor designs to achieve high-purity CO_2, syngas and/or hydrogen production for power or chemical applications. The development of optimal chemical looping processes requires understanding the fuel-metal oxide contacting pattern, transport phenomena occurring within the reactor, and the kinetics of the chemical reactions occurring between the fuel and the oxygen carrier. System integration, particularly with respect to parasitic energy consumption, is also an important part of the process optimization. The attrition behavior of the oxygen carriers and the *in situ* ash removal are additional factors that need to be included in the process design. The main challenge,

however, is on the reaction viability, physical strength, and the cost of the oxygen carriers for sustainable chemical looping operation and the eventual successful process commercialization. With continued efforts to optimize and successfully demonstrate large-scale test units, the chemical looping technology has a high potential to become a future carbon mitigation method.

ACKNOWLEDGMENT

The authors would like to acknowledge William Wang for his assistance in the preparation of the manuscript.

REFERENCES

1. Ishida M, Zheng D, Akehta T. Evaluation of a chemical looping combustion power generation system by graphic energy analysis. *Energy* 1987a, 12:147–154.
2. Messerschmitt A. Process for producing hydrogen. US Patent No. 971,206, 1910.
3. Lane H. Process for the production of hydrogen. US Patent No. 1,078,686, 1913.
4. Lewis WK, Gilliland EW. Production of pure carbon dioxide. US Patent No. 2,665,972, 1954.
5. Vitousek PM. Beyond global warming: Ecology and global change. *Ecology* 1994, 75:1861–1876.
6. Solomon S, Plattner G-K, Knutti R, Friedlingstein P. Irreversible climate change due to carbon dioxide emissions. *Proc Natl Acad Sci USA* 2009, 106:1704–1709.
7. British Petroleum. *BP Statistical Review of World Energy*. London: British Petroleum; 2013.
8. Edwards PP, Kuznetsov VL, David WIF, Brandon NP. Hydrogen and fuel cells: towards a sustainable energy future. *Energy Policy* 2008, 36:4356–4362.
9. Dufour J, Serrano DP, Galvez JL, Moreno J, Gonzalez A. Hydrogen production from fossil fuels: life cycle assessment of technologies with low greenhouse gas emissions. *Energy Fuels* 2011, 25:2194–2202.
10. Meerman JC, Hamborg ES, van Keulen T, Ramirez A, Turkenburg WC, Faaij APC. Techno-economic assessment of CO_2 capture at steam methane reforming facilities using commercially available technology. *Int J Greenhouse Gas Control* 2012, 9:160–171.
11. Abbas HF, Wan Daud WMA. Hydrogen production by methane decomposition: a review. *Int J Hydrogen Energy* 2010, 35:1160–1190.
12. Richter H, Knoche K. Reversibility of combustion processes: efficiency and costing. In: *ACS Symposium Series* 235, American Chemical Society, Washington, DC, 1983, 71–85.
13. Anheden M. Analysis of gas turbine systems for sustainable energy conversion. PhD Thesis, Royal Institute of Technology, 2000.
14. Connell DP, Dunkerley ML, Lewandowski DA, Zeng L, Wang D, Fan L-S, Statnick RM. Techno-economic analysis of a coal direct chemical looping power plant with carbon dioxide capture. In: *Proceedings of the 37th International Technical Conference on Clean Coal & Fuel Systems*, Clearwater, FL, June 3–7, 2012
15. Dean CC, Blamey J, Florin NH, Al-Jeboori MJ, Fennell PS. The calcium looping cycle for CO_2 capture from power generation, cement manufacture and hydrogen production. *Chem Eng Res Des* 2011, 89: 836–855.
16. Fan L-S, Zeng L, Wang W, Luo S. Chemical looping processes for CO_2 capture and carbonaceous fuel conversion – prospect and opportunity. *Energy Environ Sci* 2012, 5:7254–7280.
17. Wang K, Yu Q, Qin Q, Duan W. Feasibility of a Co oxygen carrier for chemical looping air separation: thermodynamics and kinetics. *Chem Eng Technol* 2014, 37:1500–1506.
18. Moghtaderi B. Review of the recent chemical looping process developments for novel energy and fuel applications. *Energy Fuels* 2012, 26:15–40.
19. Irfan MF, Usman MR, Kusakabe K. Coal gasification in CO_2 atmosphere and its kinetics since 1948: a brief review. *Energy* 2011, 36:12–40.
20. Molina A, Mondragon F. Reactivity of coal gasification with steam and CO_2. *Fuel* 1998, 77:1831–1839.
21. Imtiaz Q, Hosseini D, Muller CR. Review of oxygen carriers for chemical looping with oxygen uncoupling (CLOU): thermodynamics, material development, and synthesis. *Energy Technol* 2013, 1:633–647.
22. Zafar Q, Abad A, Mattisson T, Gevert B, Strand M. Reduction and oxidation kinetics of Mn_3O_4/Mg–ZrO_2 oxygen carrier particles for chemical-looping combustion. *Chem Eng Sci* 2007, 62:6556–6567.
23. Ryden M, Lyngfelt A, Mattisson T. $CaMn_{0.875}Ti_{0.125}O_3$ as oxygen carrier for chemical-looping combustion with oxygen uncoupling (CLOU)—experiments in a continuously operating fluidized-bed reactor system. *Int J Greenhouse Gas Control* 2011, 5:356–366.
24. Mattisson T, Leion H, Lyngfelt A. Chemical-looping with oxygen uncoupling using CuO/ZrO_2 with petroleum coke. *Fuel* 2009, 88:683–690.

25. Doctor R, Palmer A, Coleman D, Davison J, Hendriks C, Kaarstad O, Ozaki M, Austell M. Transport of CO_2. In: Metz B, Davidson O, de Coninck HC, Loos M, Meyer LA, eds. *IPCC Special Report on Carbon Dioxide Capture and Storage*; 2005.
26. Fan L-S. *Chemical Looping Systems for Fossil Energy Conversions*. Hoboken, NJ: John Wiley and Sons; 2010.
27. Tong A, Bayham S, Kathe M, Zeng L, Luo S, Fan L-S. Iron-based syngas chemical looping process and coal-direct chemical looping process development at Ohio State University. *Appl Energy* 2014, 113:1836–1845.
28. Lyngfelt A, Leckner B. A 1000 MW_{th} chemical-looping combustor for solid fuels—discussion of design and costs. In: *Proceedings of the 3rd International Conference on Chemical Looping*, Gothenburg, Sweden, September 9–11, 2014.
29. Jiang P, Wei F, Fan L-S. General approaches to reactor design. In: Yang W-C, ed. *Handbook of Fluidization and Fluid-Particle Systems*. New York, NY: Marcel Decker Inc.; 2003.
30. Sozinho T, Pelletant W, Stainton H, Guillou F, Gauthier T. Main results of the 10 kW_{th} pilot plant operation. In: *Proceedings of the 2nd International Chemical Looping Conference*, Darmstadt, Germany, September 26–28, 2012.
31. Kolbitsch P, Bolhar-Nordenkampf J, Proll T, Hofbauer H. Operating experience with chemical looping combustion in a 120 kW dual circulating fluidized bed (DCFB) unit. *Int J Greenhouse Gas Control* 2010a, 4:180–185.
32. Lyngfelt A, Thunman H. Construction and 100 h of operational experience of a 10-kW chemical looping combustor. In: Thomas D, ed. *Carbon Dioxide Capture for Storage in Deep Geologic Formations—Results from the CO_2 Capture Project*, vol. 1. London, UK: Elsevier Science; 2005, 625–645.
33. Adanez J, Gayan P, Celaya J, de Diego L, Garcia-Labiano F, Abad A. Chemical looping combustion in a 10 kW_{th} prototype using a CuO/Al_2O_3 oxygen carrier: effect of operating conditions on methane combustion. *Ind Chem Eng Res* 2006, 45:6075–6080.
34. Forero CR, Gayan P, de Diego LF, Abad A, Garcia-Labiano F, Adanez J. Syngas combustion in a 500 W_{th} chemical-looping combustion using an impregnated Cu-based oxygen carrier. *Fuel Proc Technol* 2009, 90:1471–1479.
35. Hallberg P, Källén M, Jing D, Snijkers F, van Noyen J, Rydén M, Lyngfelt A. Experimental investigation of $CaMnO_{[3-\delta]}$ based oxygen carriers used in continuous chemical-looping combustion. *Int J Chem Eng* 2014, vol. 2014, Article ID 412517, 9 pages. doi:10.1155/2014/412517.
36. Proll T, Kolbitsch P, Bolhar-Nordenkampf J, Hofbauer H. A novel dual circulating fluidized bed system for chemical looping processes. *AIChE J* 2009a, 55:3255–3266.
37. Son SR, Kim SD. Chemical looping combustion with NiO and Fe_2O_3 in a thermobalance and circulating fluidized bed reactor with double loops. *Ind Eng Chem Res* 2006, 45:2689–2696.
38. Ryu H-J, Jin G-T, Yi C-K. Demonstration of inherent CO_2 separation and no NO_x emission in a 50 kW_{th} chemical looping combustor: continuous reduction and oxidation experiment. In: *7th International Conference on Greenhouse Gas Control Technologies*, Vancouver, Canada, 2004, 1907–1910.
39. Linderholm C, Lyngfelt A, Cuadrat A, Jerndal E. Chemical-looping combustion of solid fuels – Operation in a 10 kW unit with two fuels, above-bed and in-bed fuel feed and two oxygen carriers, manganese ore and ilmenite. *Fuel* 2012, 102:808–822.
40. Abad A, Adanez-Rubio I, Gayan P, Garcia-Labiano F, de Diego LF, Adanez J. Demonstration of chemical-looping with oxygen uncoupling (CLOU) process in a 1.5 kW_{th} continuously operating unit using a Cu-based oxygen-carrier. *Int J Greenhouse Gas Control* 2012, 6:189–200.
41. Markstrom P, Linderholm C, Lyngfelt A. Operation of a 100 kW chemical-looping combustor with Mexican petroleum coke and Cerrejon coal. *Appl Energy* 2014, 113:1830–1835.
42. Strohle J, Orth M, Epple B. Design and operation of a 1 MW_{th} chemical looping pilot. *Appl Energy* 2014a, 113:1490–1495.
43. Perez-Vega R, Abad A, de Diego LF, Garcia-Labiano F, Gayan P, Adanez J. Design of a 50 kW_{th} CLC pilot plant with solid fuels. In: *Proceedings of the 3rd International Chemical Looping Conference*, Gothenburg, Sweden, September 9–11, 2014.
44. Thon A, Kramp M, Hartge E-U, Heinrich S, Werther J. Operational experience with a system of coupled fluidized beds for chemical looping combustion of solid fuels using ilmenite as oxygen carrier. *Appl Energy* 2014, 118:309–317.
45. Bayham SC, Kim HR, Wang D, Tong A, Zeng L, McGiveron O, Kathe MV, Chung E, Wang W, Wang A, et al. Iron-based coal direct chemical looping combustion process: 200 h continuous operation of a 25-kW_{th} subpilot unit. *Energy Fuels* 2013, 27:1347–1356.
46. Kim HR, Wang D, Zeng L, Bayham S, Tong A, Chung E, Kathe MV, Luo S, McGiveron O, Wang A, et al. Coal direct chemical looping combustion process: Design and operation of a 25-kW_{th} sub-pilot unit. *Fuel* 2013, 108:370–384.
47. Song Q, Xiao R, Deng Z, Zheng W, Shen L, Xiao J. Multicycle study on chemical-looping combustion of simulated coal gas with a CaSO4 oxygen carrier in a fluidized bed reactor. *Energy Fuels* 2008, 22:3661–3672.

48. Adánez J, de Diego LF, García-Labiano F, Gayán P, Abad A, Palacios J. Selection of oxygen carriers for chemical-looping combustion. *Energy Fuels* 2004, 18:371–377.
49. Peterson SB, Konya G, Clayton CK, Lewis RJ, Wilde BR, Eyring EM, Whitty KJ. Characteristics and CLOU performance of a novel SiO_2-supported oxygen carrier prepared from CuO and β-SiC. *Energy Fuels* 2013, 27:6040–6047.
50. Johansson M, Mattisson T, Lyngfelt A. Use of $NiO/NiAl_2O_4$ particles in 10 kW chemical looping combustor. *Ind Eng Chem Res* 2006, 45:5911–5919.
51. Linderholm C, Mattisson T, Lyngfelt A. Long-term integrity testing of spray-dried particles in a 10-kW chemical-looping combustor using natural gas as fuel. *Fuel* 2009, 88:2083–2096.
52. Hallberg P, Rydén M, Mattisson T, Lyngfelt A. $CaMnO_{3-\delta}$ made from low cost material examined as oxygen carrier in chemical-looping combustion. *Energy Procedia* 2014, 63:80–86.
53. Kallën M, Ryden M, Dueso C, Mattisson T, Lyngfelt A. $CaMn_{0.9}Mg_{0.1}O_{3-\delta}$ as oxygen carrier in a gas-fired 10 kW_{th} chemical-looping combustion unit. *Ind Eng Chem Res* 2013, 52:6923–6932.
54. Kolbitsch P, Bolhàr-Nordenkampf J, Pröll T, Hofbauer H. Comparison of two Ni-based oxygen carriers for chemical looping combustion of natural gas in 140 kW continuous looping operation. *Ind Eng Chem Res* 2009, 48:5542–5547.
55. Proll T, Mayer K, Bolhar-Nordenkamph J, Kolbitsch P, Mattisson T, Lyngfelt A, Hofbauer H. Natural minerals as oxygen carriers for chemical looping combustion in a dual circulating fluidized bed system. *Energy Procedia* 2009b, 1:27–34.
56. Berguerand N, Lyngfelt A, Mattisson T, Markstrom P. Chemical looping combustion of solid fuels in a 10 kW_{th} unit. *Oil Gas Sci Technol* 2011, 66:181–191.
57. Berguerand N, Lyngfelt A. Chemical-looping combustion of petroleum coke using ilmenite in a 10 kW_{th} unit—high temperature operation. *Energy Fuels* 2009, 23:5257–5268.
58. Linderholm C, Lyngfelt A, Dueso C. Chemical looping combustion of solid fuels in a 10 kW reactor system using natural minerals as oxygen carrier. *Energy Procedia* 2013, 37:598–607.
59. Markstrom P, Lyngfelt A. Designing and operating a cold-flow model of a 100 kW chemical-looping combustor. *Powder Technol* 2012, 222:182–192.
60. Markstrom P, Linderholm C, Lyngfelt A. Operation of a 100kW chemical-looping combustor with Mexican petroleum coke and Cerrejon coal. In: *Proceedings of the 2nd International Chemical Conference*, Darmstadt, Germany, September 26–28, 2012.
61. Markstrom P, Linderholm C, Lyngfelt A. Chemical looping combustion of solid fuels—design and operation of a 100 kW unit with bituminous coal. *Int J Greenhouse Gas Control* 2013, 15:150–162.
62. Shen L, Wu J, Xiao J. Experiments on chemical looping combustion of coal with a NiO based oxygen carrier. *Combust Flame* 2009a, 156:721–728.
63. Shen L, Wu J, Xiao J, Song Q, Xiao R. Chemical looping combustion of biomass in a 10kW_{th} reactor with iron oxide as an oxygen carrier. *Energy Fuels* 2009b, 23:2498–2505.
64. Gu H, Shen L, Xiao J, Zhang S, Song T. Chemical looping combustion of biomass/coal with natural iron ore as oxygen carrier in a continuous reactor. *Energy Fuels* 2011, 25:446–455.
65. Shen L, Wu J, Gao Z, Xiao J. Characterization of chemical looping combustion of coal in a 1 kW_{th} reactor with a nickel-based oxygen carrier. *Combust Flame* 2010, 157:934–942.
66. Gu H, Shen L, Niu X, Ge H, Zhong Z. Cement/CaO-decorated iron ore as oxygen carrier for chemical looping combustion of coal. In: *Proceedings of the 3rd International Chemical Looping Conference*, Gothenburg, Sweden, September 9–11, 2014.
67. Niu X, Shen L, Gu H, Song T. Performance of chemical looping combustion of sewage sludge and phosphorus migration based on hematite oxygen carrier in a 1 kW_{th} reactor. In: *Proceedings of the 3rd International Chemical Looping Conference*, Gothenburg, Sweden, September 9–11, 2014.
68. Adanez-Rubio I, Abad A, Gayan P, García-Labiano F, de Diego LF, Adánez J. The fate of sulphur in the Cu-based chemical looping with oxygen uncoupling (CLOU) process. *Appl Energy* 2014, 113:1855–1862.
69. Cuadrat A, Abad A, Garcia-Labiano F, Gayán P, de Diego LF, Adánez J. The use of ilmenite as oxygen-carrier in a 500 W_{th} chemical-looping coal combustion unit. *Int J Greenhouse Gas Control* 2011, 5:1630–1642.
70. Strohle J, Orth M, Epple B. Chemical looping combustion of hard coal in a 1 MW_{th} pilot plant using ilmenite as oxygen carrier. In: *Proceedings of the 3rd International Chemical Looping Conference*, Gothenburg, Sweden, September 9–11, 2014b.
71. Li F, Zeng L, Fan L-S. Biomass direct chemical looping: process simulation. *Fuel* 2010a, 89:3773–3784.
72. Li F, Zeng L, Velazquez-Vargas L, Yoscovits Z, Fan L-S. Syngas chemical looping gasification process: bench scale studies and reactor simulations. *AIChE J* 2010b, 56:2186–2199.
73. Erlach B, Schmidt M, Tsatsaronis G. Comparison of carbon capture IGCC with pre-combustion decarbonisation and with chemical-looping combustion. *Energy* 2011, 36:3804–3815.
74. Rezvani S, Huang Y, McIlveen-Wright D, Hewitt N, Mondol JD. Comparative assessment of coal fired IGCC systems with CO_2 capture using physical

absorption, membrane reactors and chemical looping. *Fuel* 2009, 88:2463–2472.

75. Anheden M, Svedberg G. Exergy analysis of chemical looping combustion systems. *Energy Convers Manag* 1998, 39:1967–1980.
76. Xiang W, Wang S. Investigation of gasification chemical looping combustion combined cycle performance. *Energy Fuels* 2008, 22:961–966.
77. Wang X, Economides M. *Advanced Natural Gas Engineering*. Houston, TX: Gulf Publishing Company; 2009.
78. Rydén M, Lyngfelt A. Using steam reforming to produce hydrogen with carbon dioxide capture by chemical-looping combustion. *Int J Hydrogen Energy* 2006, 31:1271–1283.
79. Tong A, Sridhar D, Sun Z, Kim HR, Zeng L, Wang F, Wang D, Kathe MV, Luo S, Sun Y, et al. Continuous high purity hydrogen generation from a syngas chemical looping 25kW$_{th}$ sub-pilot unit with 100% carbon capture. *Fuel* 2013, 103:495–505.
80. Cormos CC. Hydrogen production from fossil fuels with carbon capture and storage based on chemical looping systems. *Int J Hydrogen Energy* 2011, 36:5960–5971.
81. Mizia F, Rossini S, Cozzolino M, Cornaro U, Tlatlik S, Kaus I, Bakken E, Larring Y. One step decarbonization. In: Eide LI, ed. *Carbon Dioxide Capture for Storage in Deep Geologic Formations*, vol. 3. Berkshire: CPL Press; 2009.
82. Kang K-S, Kim C-H, Bae K-K, Cho W-C, Jeong S-U, Lee Y-J, Park C-S. Reduction and oxidation properties of Fe_2O_3/ZrO_2 oxygen carrier for hydrogen production. *Chem Eng Res Des* 2014, 92(11):2584–2597.
83. Nakamura T. Hydrogen production from water utilizing solar heat at high temperatures. *Solar Energy* 1977, 19:467–475.
84. Svoboda K, Siewiorek A, Baxter D, Rogut J, Pohorely M. Thermodynamic possibilities and constraints for pure hydrogen production by a nickel and cobalt-based chemical looping process at lower temperatures. *Energy Convers Mgmt* 2008, 49:221–231.
85. Svoboda K, Slowinski G, Rogut J, Baxter D. Thermodynamic possibilities and constraints for pure hydrogen production by iron based chemical looping process at lower temperatures. *Energy Convers Manag* 2007, 48:3063–3073.
86. Xue Z, Chen S, Wang D, Xiang W. Design and fluid dynamic analysis of a three-fluidized-bed reactor system for chemical-looping hydrogen generation. *Ind Eng Chem Res* 2012, 51:4267–4278.
87. Muenster P, Grabke HJ. Kinetics of the steam reforming of methane with iron, nickel, and iron-nickel alloys as catalysts. *J Catalysis* 1981, 72:279–287.
88. Luo S, Zeng L, Xu D, Kathe M, Chung E, Deshpande N, Qin L, Majumder A, Hsieh T-L, Tong A, et al. Shale gas-to-syngas chemical looping process for stable shale gas conversion to high purity syngas with a H_2:CO ratio of 2:1. *Energy Environ Sci* 2014, 7:4104–4117.
89. Ehrensberger K, Frei A, Kuhn P, Oswald HR, Hug P. Comparative experimental investigations of the water-splitting reaction with iron oxide $Fe_{1-y}O$ and iron manganese oxides $(Fe_{1-x}Mn_x)_{1-y}O$. *Solid State Ion* 1995, 78:151–160.
90. Alvani C, Ennas G, La Barbera A, Marongiu G, Padella F, Varsano F. Synthesis and characterization of nanocrystalline $MnFe_2O_4$: advances in thermochemical water splitting. *Int J Hydrogen Energy* 2005, 30:1407–1411.
91. Pena JA, Lorente E, Romero E, Herguido J. Kinetic study of the redox process for storing hydrogen reduction stage. *Catal Today* 2006, 116:439–444.
92. Cleeton JPE, Bohn CD, Müller CR, Dennis JS, Scott SA. Different methods of manufacturing Fe-based oxygen carrier particles for reforming via chemical looping, and their effect on performance. In: Yue G, Zhang H, Zhao C, Luo Z, eds. *Proceedings of the 20th International Conference on Fluidized Bed Combustion*, Xi'an, China, 2009, 505–511R.
93. Hacker V, Fankhauser R, Faleschini G, Fuchs H, Friedrich K, Muhr M, Kordesch K. Hydrogen production by steam-iron process. *J Power Sources* 2000, 86:531–535.
94. Thalera M, Hackera V, Anilkumara M, Alberinga J, Besenharda JO, Schröttnerb H, Schmiedb M. Investigations of cycle behaviour of the contact mass in the RESC process for hydrogen production. *Int J Hydrogen Energy* 2006, 31:2025–2031.
95. Sridhar D, Tong A, Kim H, Zeng L, Li F, Fan L-S. Syngas chemical looping process: design and construction of a 25 kW$_{th}$ subpilot unit. *Energy Fuels* 2012, 26:2292–2302.
96. Tong A, Zeng L, Kathe MV, Sridhar D, Fan L-S. Application of the moving-bed chemical looping process for high methane conversion. *Energy Fuels* 2013b, 27:4119–4128.
97. Lewis WK, Gilliland ER, Reed WA. Reaction of Methane with Copper Oxide in a Fluidized Bed. *Ind Eng Chem* 1949, 41:1227–1237.
98. Ryden M, Lyngfelt A, Mattisson T. Synthesis gas generation by chemical-looping reforming in a continuously operating laboratory reactor. *Fuel* 2006, 85:1631–1641.
99. Pröll T, Bolhàr-Nordenkampf J, Kolbitsch P, Hofbauer H. Syngas and a separate nitrogen/argon stream via chemical looping reforming—a 140 kW pilot plant study. *Fuel* 2010, 89:1249–1256.
100. de Diego LF, Ortiz M, García-Labiano F, Adánez J, Abad A, Gayán P. *J Power Sources* 2009, 192:27–34.
101. Chiesa P, Lozzaa G, Malandrinob A, Romanoa M, Piccolob V. Three-reactors chemical looping process

for hydrogen production. *Int J Hydrogen Energy* 2008, 33:2233–2245.

102. Rath L. Assessment of hydrogen production with CO_2 capture—volume 1: baseline state-of-the-art plants. National Energy Technology Laboratories Technical Report, DOE/NETL-2010-1434, 2010.
103. Shuster E. Analysis of natural gas-to-liquid transportation fuels via Fischer-Tropsch. National Energy Technology Laboratories Technical Report, DOE/NETL-2013/1597, 2013.
104. Turner MJ. Quality guidelines for energy system studies: capital cost scaling methodology. National Energy Technology Laboratories Technical Report, NETL/DOE-341/013113, 2013.
105. Chou V, Kearins D, Turner M, Woods M, Zoelle A. Quality guidelines for energy system studies: process modeling design parameters. National Energy Technology Laboratories Technical Report, DOE/NETL-2014/051314, 2014.
106. Myles P, Lanka S, Lu Y. Quality guidelines for energy system studies: specification for selected feedstocks. National Energy Technology Laboratories Technical Report, DOE/NETL-341/011812, 2012.
107. Xiao R, Song Q, Song M, Lu Z, Zhang S, Shen L. Pressurized chemical-looping combustion of coal with an iron ore-based oxygen carrier. *Combust Flame* 2011, 157:1140–1153.
108. Xiao R, Chen L, Sara C, Zhang S, Bhattacharya S. Pressurized chemical-looping combustion of coal using an iron ore as oxygen carrier in a pilot-scale unit. *Int J Greenhouse Gas Control* 2012, 10: 363–373.
109. Ma J, Zhao H, Tian X, Wei Y, Rajendran S, Zhang Y, Bhattacharya S, Zheng C. Chemical looping combustion of coal in a 5 kW_{th} interconnected fluidized bed reactor using hematite as oxygen carrier. In: *Proceedings of the 3rd International Conference on Chemical Looping*, Gothenburg, Sweden, September 9–11, 2014.
110. Abdulally I. Alstom's chemical looping combustion proto-type for CO_2 capture from existing pulverized coal-fired power plants. In: *Proceedings of Department of Energy National Energy Technology Laboratory CO_2 Capture Technology Meeting*, Pittsburgh, PA, 2011.

